IEEE Access
Multidisciplinary ⋮ Rapid Review ⋮ Open Access Journal

Received 4 February 2023, accepted 25 February 2023, date of publication 20 March 2023, date of current version 3 April 2023.

Digital Object Identifier 10.1109/ACCESS.2023.3259720

RESEARCH ARTICLE

Extended Approach to Analytical Triangular Decoupling Internal Model Control of Square Stable Multivariable Systems With Delays and Right-Half-Plane Zeros

KOLAWOLE S. OGUNBA[1], AFEEZ A. FAKUNLE[1], TOKUNBO OGUNFUNMI[1], AND OLUWAFEMI TAIWO[2]

[1]Department of Electrical and Computer Engineering, Santa Clara University, Santa Clara, CA 95053, USA
[2]Process System Engineering Laboratory, Department of Chemical Engineering, Obafemi Awolowo University, Ife, Osun 220282, Nigeria

Corresponding author: Kolawole S. Ogunba (kogunba@scu.edu)

This work was supported in part by the Alexander von Humboldt Foundation Fund, and in part by the Santa Clara University School of Engineering Inclusive Excellence Postdoctoral Fellowship for 2022/2023 Session.

ABSTRACT The Analytical Triangular Decoupling Internal Model Control (ATDIMC) technique for 2×2 systems is generalized to $n \times n$ systems ($n \geq 2$) with delays and right-half-plane (RHP) transmission zeros. The formulation is done by first creating a triangular closed-loop transfer function matrix corresponding to the achievement of the triangular decoupling objective of restraining inverse-response and control-loop-interaction characteristics to a single plant output. Subsequently, the corresponding multivariable internal model controller is calculated, with transfer-function approximations made using an optimization algorithm that minimizes the Integral Time-Weighted Absolute Error (ITAE) of the difference between the step responses of the original and reduced expressions. It is shown that n ATDIMC designs emerge that achieve the shifting of inverse responses and interactions to a least-desired output, with delays retained for all outputs and asymptotic tracking of setpoints achieved for all n outputs of each design. To mitigate the possible effect of severe interaction on the least-desired output, a modification of this formulation is performed to spread inverse-response behavior to a second output, while minimizing the interaction of that output with the initial least-desired output. Simulation results for selected 3×3 and 4×4 systems show the effectiveness of these propositions.

INDEX TERMS Triangular decoupling, multivariable systems, multi-input, multi-output systems, square systems, open-loop-stable systems, nonminimum-phase systems, RHP transmission zeros, internal model control, input delays, model simplification.

I. INTRODUCTION

Internal Model Control (IMC) explicitly includes the mathematical model of an open-loop-stable plant in the control structure for the plant, hence the name. Originally formulated for open-loop-stable, Single-Input, Single-Output (SISO) dynamical systems, the IMC configuration combines cascade, parallel and feedback connections in a single configuration to achieve such desired characteristics as design simplicity, closed-loop stability guarantee, null steady-state-offset guarantee and transparency of robust design [1], [2], [3]. The IMC structure contains a parallel combination of the plant and its model, with the controller being the exact inverse (for minimum-phase systems) or approximate inverse (for nonminimum-phase systems) of the model of the controlled system. Extended formulations of, or modifications of the SISO IMC concept have been made and applied to several control situations, including PID control [3], [4], control of unstable systems [3], [5], [6], control of nonlinear systems [7], [8], control

The associate editor coordinating the review of this manuscript and approving it for publication was Xiwang Dong.

of square multivariable systems [3], [9] and decentralized control [3], [10].

In respect of the extension of SISO IMC to square nonminimum-phase Multiple-Input, Multiple-Output (MIMO) systems without delays, the model of the plant is first factorized into the ''good'' factor without RHP transmission zeros and ''bad'' factor with RHP transmission zeros, with the ''good'' factor subsequently inverted and augmented with a filter matrix for properness. There are theoretically infinite possibilities of factorization results for a nonminimum-phase transfer function matrix, and this implies that a closed-loop transfer function matrix must be directly or indirectly specified for a particular factorization process before a corresponding factorization can be done. Different choices of the closed-loop transfer function matrix have led to a variety of outcomes in respect of degrees of allowed control-loop interactions and inverse responses, leading to such outcomes as dynamic decoupling, triangular decoupling and optimal spread of inverse responses and control-loop interactions [2], [3], [9].

The extension of SISO IMC to square MIMO systems with delays has not been straightforward because the zero polynomial of a square transfer function matrix with delays is irrational, complicating the process of inversion of the matrix. However, with the specification of a diagonal closed-loop transfer function matrix and the determination of the internal model controller that approximately yields such a matrix, it has been shown that Internal Model Control that achieves dynamic decoupling can be developed for square MIMO systems with delays, hence the emergence of ''Decoupling Internal Model Control'' (DIMC) [11], [12], [13], [14], [15]. For square MIMO systems with delays and without RHP transmission zeros, the process of design of controllers using DIMC involves approximate transfer function matrix inversion, with appropriate elements of the resulting controller matrix approximated to rational transfer functions with delays [11], [12], [14]. Because of the intuitive appeal of dynamic decoupling [16], many multivariable control formulations have been developed over the years using the dynamic decoupling concept, with IMC either used directly or together with such concepts such as Simplified Decoupling and Inverted Decoupling achieve control using an IMC structure or a conventional feedback structure ([15], [17], [18], [19], [20], [21], [22], [23], [24]).

For systems with delays and RHP transmission zeros, transfer function matrix inversion leads to instability. To actualize DIMC for such systems without introducing instability, the desired diagonal closed-loop transfer function matrix is utilized using a procedure similar to that of the aforementioned dynamic-decoupling-based MIMO IMC for delay-free nonminimum-phase (NMP) systems [11], [14]. The all-pass form of the elements of the diagonal of this matrix ensures that the RHP poles of the approximately inverted matrix of the plant can be removed, yielding a closed-loop stability guarantee, but with the inevitable spread of inverse responses to all outputs [11], [14], [25].

While dynamic-decoupling-based IMC achieves setpoint-tracking and disturbance-rejection objectives, it has been shown in [25] and [26] that a triangular-decoupling-based formulation offers the possibility of achieving a better overall performance-index value than a dynamic-decoupling-based formulation for a delay-free system with RHP transmission zeros. It has also been shown in [25] and [26] that in comparison to dynamic decoupling, better results can be produced using triangular decoupling for nonminimum-phase systems with strong control-loop interactions and in situations where there are control objectives that prioritize the performance of some outputs over others. The main motivation of this study is therefore provided by the possibility of the extension of the aforementioned advantages to MIMO IMC design for square MIMO systems with delays and RHP transmission zeros.

Over the last five decades, several authors have provided solutions to different formulations of the triangular decoupling problem using a variety of methods of analysis and design. By using desired upper-triangular and lower-triangular closed-loop transfer function matrices, the triangular decoupling problem was solved in [25] and [26] for delay-free multivariable systems with RHP transmission zeros such that inverse responses and interactions are shifted to a single, least-desired output. In [27], a geometric formulation was used to achieve state-feedback-based triangular decoupling for multivariable systems. By modifying Silverman's inversion algorithm and using it for the triangular decoupling problem as formulated in state space, it was shown in [28] that the existence of state feedback laws for triangular decoupling was equivalent to conditions for invertibility. In [29], an algebraic technique was used to determine conditions for existence of solution to triangular decoupling problem, with a proposed pole-placement-based controller design method providing the solution to the triangular decoupling problem. In [30], the regular controllability distributions were used in achieving triangular decoupling in nonlinear multivariable systems. Robust input-output triangular decouplers were developed in [31] for linear multivariable systems with nonlinear uncertain structures. Realizable proportional state feedback was utilized in [32] for triangular decoupling of multivariable systems with delays. The argument was made in [33] of the equivalence of the triangular-diagonal-dominance and coprime factorization-based conditions for existence of solution to the triangular decoupling problem. The canonical decomposition technique of a right invertible system was used in [34] to obtain solutions to the triangular decoupling problem, with explicit solutions obtained using the pole assignment technique. In [35], static feedback was used to solve the triangular decoupling problem by establishing necessary and sufficient conditions for triangular decoupling numerically and then using an algorithm to develop triangularly decouplable partitions. Necessary and sufficient conditions for solvability of the so-called ''Triangular-Decoupling-with-Disturbance-Rejection (TDDR) problem'' were derived in [36] for neutral time-delay systems, with the problem subsequently solved

using controllers without delays. The DIMC technique of [14] was modified in [37] to achieve triangular decoupling for 2×2 systems with delays and single RHP zeros, leading to the creation of the "Analytical Triangular Decoupling Internal Model Control" (ATDIMC) strategy.

Of the above formulations, the techniques of [25] and [26] were presented in the Laplace domain and therefore offer the simplest and most direct procedure for using transfer function matrices to extend the triangular decoupling IMC concept to square MIMO systems with delays and RHP zeros, while explicitly addressing the matter of shifting of both inverse responses and control-loop interactions to a single output. While the DIMC technique of [14] was modified into ATDIMC to achieve triangular decoupling in [37] for 2×2 systems with delays and RHP zeros, it can be argued that ATDIMC is also equivalently the result of a reformulation of delay-free triangular-decoupling-based IMC in [25] to achieve triangular decoupling for 2×2 systems with delays and RHP zeros. The formulation of [37] stands as the only one to date that tackles the triangular decoupling problem for square multivariable systems with delays and RHP zeros using the IMC structure. Since it was successfully shown in [37] for 2×2 systems that the nominal and robustness characteristics of at least one of the ATDIMC designs for each considered system were better than those obtained using DIMC, a motivation is provided for generalizing the ATDIMC technique of [37] to $n \times n$ systems with delays and RHP transmission zeros ($n > 2$). If the generalization is successful, ATDIMC can be presented as a better technique of achieving control objectives than the existing DIMC for square multivariable systems with delays and RHP zeros.

In this study, the ATDIMC concept in [37] was extended to $n \times n$ systems with delays and single RHP transmission zeros. The closed-loop transfer function matrix corresponding to the shifting of the inverse response and control-loop interaction characteristics to the nth output is first developed, and the corresponding internal model controller is computed, with provisions made to ensure that closed-loop stability is guaranteed. Subsequently, the closed-loop transfer function matrix corresponding to the shift of the inverse responses and control-loop interactions to the ith output ($i < n$) was also developed, and the corresponding controller was developed. Both formulations yield n ATDIMC designs for an $n \times n$ system. Because of the possibility of severe interaction added to the least-desired output, a modified ATDIMC formulation was performed to remove the interaction effect of an output y_k on the least-desired output y_w, $w \neq k$, with an inverse response placed on y_k. Simulation results, including those from designs on the model of a practical 3×3 Depropanizer in [13], show the effectiveness of the propositions.

The remainder of this paper is organized as follows. Section II-A provides the mathematical preliminaries that define the closed-loop transfer function matrix of a continuous-time square stable multivariable system within the IMC configuration under the assumption of a perfect plant-model match and in the absence of disturbances. Section II-B defines triangular

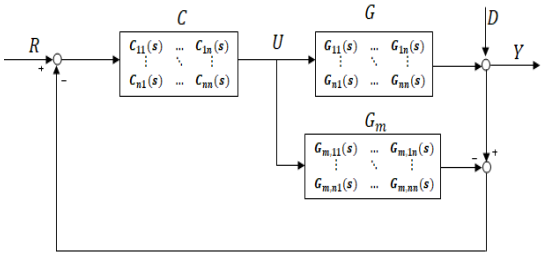

FIGURE 1. Block diagram of internal model control for square MIMO systems.

transfer function matrices, including those that are technically not triangular matrices but can emerge as triangular matrices if the variables that are related by such matrices are rearranged. Sections III-A and III-B develop the internal model controller equations within the ATDIMC framework that restrict inverse response and control-loop interaction characteristics to the nth and ith outputs respectively ($i < n$). Sections III-C and III-D develop internal model controller equations within the modified ATDIMC framework that modify the designs of Sections III-A and III-B such that inverse responses are restricted to two outputs, and interaction contributions to the respective least-desired outputs are reduced by one. Section IV provides the technique for minimization of the Integral Time-Weighted Absolute Error (ITAE) of the difference between the original and reduced transfer function expressions as a technique for the reduction of the elements of the internal model controllers developed in Section III. Section V discusses the analysis of the designed controllers for robust stability and performance using μ-analysis. The simulation results are presented and discussed in Section VI, and conclusions are presented in Section VII. The Appendices Section gives details of the proofs of Propositions 1 and 2 (of Sections III-A and III-C respectively) and the designed controllers of Section VI, while the cited publications are listed in the References Section.

II. MATHEMATICAL PRELIMINARIES

A. THE MIMO IMC CONFIGURATION

Figure 1 shows a block diagram of IMC for an $n \times n$ system. The sub-systems G, G_m, and C are $n \times n$ transfer function matrices representing the plant, the model of the plant and the controller respectively. The vectors $\boldsymbol{R}$, $\boldsymbol{U}$, $\boldsymbol{D}$ and $\boldsymbol{Y}$ are the Laplace transforms of the n-sized vectors of the command signal, plant input, output disturbance and plant output respectively. The transform of the feedback signal is equal to the disturbance transform $\boldsymbol{D}$ if there is a perfect plant-model match.

Both $\boldsymbol{R}$ and $\boldsymbol{D}$ in Figure 1 are assumed to be transforms of vectors of positive unit step and negative unit step functions respectively. Mathematically, if $\mu(t)$ is a unit step function such that

$$\mu(t) = \left.\begin{array}{ll} 0, & t < 0 \\ 1, & t \geq 0 \end{array}\right\} \tag{1}$$

then $\boldsymbol{R}$ and $\boldsymbol{D}$ can be written as

$$\boldsymbol{R}(s) = \begin{bmatrix} \mu(t - t_{r,1}) & \mu(t - t_{r,2}) & \dots & \mu(t - t_{r,n}) \end{bmatrix}^T \tag{2}$$

$$\boldsymbol{D}(s) = \begin{bmatrix} -\mu(t - t_{d,1}) & -\mu(t - t_{d,2}) & \dots & -\mu(t - t_n) \end{bmatrix}^T \tag{3}$$

where $t_{r,i} (i = 1, 2, \dots, n)$ is a constant and is chosen to allow the evaluation of the amount of interaction that the setpoint tracking in the ith loop has with all other $n - 1$ loops, and $t_{d,j} (j = 1, 2, \dots, n)$ is also a constant and is chosen to allow the evaluation of the amount of interaction that the disturbance rejection in the jth loop has with all other $n - 1$ loops.

Using multiple system reduction techniques for multivariable systems [16], the closed-loop transfer function matrix can be written as

$$Y(s) = GC(I + [G - G_m]C)^{-1}\boldsymbol{R} + \{I - G_m C\}(I + [G - G_m]C)^{-1}\boldsymbol{D}. \tag{4}$$

As stated in [37], without loss of generality, if a perfect plant-model match and the absence of disturbance are assumed, Eq. (4) becomes

$$Y(s) = G(s)C(s)R(s) \tag{5}$$

such that the closed-loop transfer function relating the plant output transform $Y(s)$ to the command signal transform $R(s)$ becomes

$$H(s) = G(s)C(s). \tag{6}$$

By implication,

$$C(s) = G^{-1}(s)H(s). \tag{7}$$

If $H(s)$ is formulated as a triangular matrix achieving triangular decoupling, then, with the inverse of $G(s)$ approximately computed, the corresponding internal model controller $C(s)$ can be found using Eq. (7), with $H(s)$ pre-set to ensure that the RHP poles of $G^{-1}(s)$ can be removed, thereby guaranteeing closed-loop stability. In addition, because the foregoing has all the features of the IMC configuration, there will be null steady-state offset and transparency of robust design through the tuning and detuning steps that perform trade-offs between performance and robustness.

B. TRIANGULAR TRANSFER FUNCTION MATRICES

Based on the definitions of upper and lower triangular matrices in [38], if an $n \times n$ matrix is defined by

$$A = \begin{bmatrix} A_{11} & A_{12} & \dots & A_{1n} \\ A_{21} & A_{22} & \dots & A_{2n} \\ \vdots & \vdots & \ddots & \vdots \\ A_{n1} & A_{n2} & \dots & A_{nn} \end{bmatrix} \tag{8}$$

then A is upper-triangular if the diagonal elements A_{ii} $(i = 1, 2, \dots, n)$ and at least one of the elements above the diagonal $(A_{12}, A_{13}, \dots, A_{1n}, A_{23}, A_{24}, \dots, A_{2n}, A_{34}, \dots, A_{3n}, \dots, A_{n-2,n-1}, A_{n-2,n}$ and $A_{n-1,n})$ are non-zero while every other element of the matrix is zero. On the other hand, A is lower-triangular if the diagonal elements and at least one of the elements below the diagonal $(A_{21}, A_{31}, A_{32}, A_{41}, A_{42}, A_{43}, \dots, A_{n-2,1}, A_{n-2,2}, \dots, A_{n-2,n-3}, A_{n1}, A_{n2}, \dots, A_{n,n-2}$ and $A_{n,n-1})$ are non-zero while every other element of the matrix is zero.

For example, the matrices A_1 and A_2 in Eqs. (9) and (10) are upper and lower 3×3 triangular transfer function matrices respectively, i.e.,

$$A_1(s) = \begin{bmatrix} \frac{2}{s+5} & \frac{3}{2s+1} & 0 \\ 0 & \frac{4}{s+5} & \frac{4}{s+7} \\ 0 & 0 & -\frac{6}{s+1} \end{bmatrix} \tag{9}$$

$$A_2(s) = \begin{bmatrix} -\frac{7}{s+4} & 0 & 0 \\ 0 & \frac{4}{2s+9} & 0 \\ \frac{5}{s+6} & \frac{8}{0.5s+1} & -\frac{1}{6s+1} \end{bmatrix}. \tag{10}$$

Let a third matrix A_3 be defined as in Eq. (11).

$$A_3(s) = \begin{bmatrix} \frac{-5}{s^2+2} & 0 & 0 \\ \frac{2}{9s+1} & \frac{4}{s+7} & \frac{9}{11s+1} \\ 0 & 0 & \frac{8}{3s+2} \end{bmatrix}. \tag{11}$$

The matrix $A_3(s)$ has a non-zero element above the diagonal (element A_{23}) and a non-zero element below the diagonal (element A_{21}). It is therefore evident that $A_3(s)$ of Eq. (11) is technically not an upper or lower triangular matrix. However, if the two 3-sized vectors $\boldsymbol{\alpha}(s)$ and $\boldsymbol{\beta}(s)$ that gave rise to $A_3(s)$ are defined as

$$\boldsymbol{\alpha}(s) = \begin{bmatrix} \alpha_1(s) & \alpha_2(s) & \alpha_3(s) \end{bmatrix}^T \tag{12}$$

$$\boldsymbol{\beta}(s) = \begin{bmatrix} \beta_1(s) & \beta_2(s) & \beta_3(s) \end{bmatrix}^T \tag{13}$$

such that

$$\alpha(s) = A_3(s).\beta(s) \tag{14}$$

then, we can re-arrange the elements of the vectors of Eqs. (12) and (13) to lead, respectively, to new vectors $\boldsymbol{\alpha}_{\boldsymbol{rearr}}(s)$ and $\boldsymbol{\beta}_{\boldsymbol{rearr}}(s)$ such that

$$\boldsymbol{\alpha}_{\boldsymbol{rearr}}(s) = \begin{bmatrix} \alpha_1(s) & \alpha_3(s) & \alpha_3(s) \end{bmatrix}^T \tag{15}$$

$$\boldsymbol{\beta}_{\boldsymbol{rearr}}(s) = \begin{bmatrix} \beta_1(s) & \beta_3(s) & \beta_2(s) \end{bmatrix}^T. \tag{16}$$

With the rearranged vectors of Eqs. (15) and (16), Eq. (14) becomes

$$\boldsymbol{\alpha}_{\boldsymbol{rearr}}(s) = A_{3,2}(s).\boldsymbol{\beta}_{\boldsymbol{rearr}}(s) \tag{17}$$

where

$$A_{3,2}(s) = \begin{bmatrix} \dfrac{-5}{s^2+2} & 0 & 0 \\ 0 & \dfrac{8}{3s+2} & 0 \\ \dfrac{2}{9s+1} & \dfrac{9}{11s+1} & \dfrac{4}{s+7} \end{bmatrix}. \quad (18)$$

Because signals within a system can be rearranged as shown in Eqs. (15), (16) and (17) without the loss of any of the features of the system, closed-loop transfer function matrices of the form of the RHS of Eq. (11) are regarded as triangular in this study.

III. GENERALIZED ATDIMC FOR SQUARE MULTIVARIABLE SYSTEMS WITH DELAYS

A. ATDIMC SHIFTING INVERSE RESPONSES AND CONTROL-LOOP INTERACTIONS TO nTH OUTPUT FOR $n \times n$ SYSTEMS WITH DELAYS AND RHP TRANSMISSION ZEROS

Let the plant and controller transfer function matrices of rational elements plus delays be respectively given by

$$G(s) = \begin{bmatrix} G_{11}(s) & \dots & G_{1n}(s) \\ \vdots & \ddots & \vdots \\ G_{n1}(s) & \dots & G_{nn}(s) \end{bmatrix} \quad (19)$$

$$C(s) = \begin{bmatrix} C_{11}(s) & \dots & C_{1n}(s) \\ \vdots & \ddots & \vdots \\ C_{n1}(s) & \dots & C_{nn}(s) \end{bmatrix} \quad (20)$$

where

$$G_{ij}(s) = G_{ijr}(s).e^{-\theta_{gij}s}; \quad i = 1, 2, \dots, n;\ j = 1, 2, \dots, n; \quad \theta_{gij} \geq 0 \quad (21)$$

$$C_{ij}(s) = C_{ijr}(s).e^{-\theta_{cij}s}; \quad i = 1, 2, \dots, n;\ j = 1, 2, \dots, n; \quad \theta_{cij} \geq 0. \quad (22)$$

In Eqs. (21) and (22), $G_{ijr}(s)$ and $C_{ijr}(s)$ are rational open-loop-stable transfer functions, and θ_{gij} and θ_{cij} are the delays associated with $G_{ij}(s)$ and $C_{ij}(s)$ respectively.

For plant inputs being $u_1, u_2, \dots, u_n$ and plant outputs being $y_1, y_2, \dots, y_n$, triangular decoupling can be achieved such that interactions and inverse responses are shifted to y_n, with outputs $y_1, y_2, \dots, y_{n-1}$ being completely non-interacting (or very mildly interacting) and without inverse responses (or with very mild inverse responses). With reference to [25], for this to occur, the closed-loop transfer function matrix $H_{n\times n,n}(s)$, assuming the existence of an RHP transmission zero at $s = z\ (z \in \mathbb{R}^+)$ for the system, can be written as

$$H_{n\times n,n}(s) = \begin{bmatrix} H_{diag1,n} & 0_{(n-1)\times 1} \\ H_{row1,n} & H_{nn} \end{bmatrix} \quad (23)$$

where

$$\left.\begin{aligned} H_{diag1,n} &= diag\left\{H_{11}, H_{22}, \dots, H_{n-1,n-1}\right\} \\ H_{row1,n} &= \begin{bmatrix} H_{n1} & H_{n2} & \cdots & H_{n,n-1} \end{bmatrix} \end{aligned}\right\} \quad (24)$$

and $0_{(n-1)\times 1}$ is an $(n-1)\times 1$ zero matrix.

In Eq. (23) and (24),

$$\left.\begin{aligned} H_{kk} &= \frac{e^{-\theta_k s}}{\tau_k s+1}; k = 1, \dots, n-1 \\ H_{np} &= \frac{s.a_{n,p}}{(s+z)}.\frac{e^{-\theta_p s}}{\tau_p s+1}; p = 1, \dots, n-1 \\ H_{nn} &= \frac{-s+z}{s+z}.\frac{e^{-\theta_n s}}{\tau_n s+1} \end{aligned}\right\}, \quad (25)$$

with $a_{n,p}$ being a constant whose value is to be calculated such that the controller in Eq. (7) is stable.

Let the adjoint of $G(s)$ be given by

$$adj(G) = \begin{bmatrix} \hat{g}_{11}(s) & \hat{g}_{12}(s) & \dots & \hat{g}_{1n}(s) \\ \hat{g}_{21}(s) & \hat{g}_{22}(s) & \dots & \hat{g}_{2n}(s) \\ \vdots & \vdots & \ddots & \vdots \\ \hat{g}_{n1}(s) & \hat{g}_{n2}(s) & \dots & \hat{g}_{nn}(s) \end{bmatrix}. \quad (26)$$

The inverse of $G(s)$ can be written as

$$G^{-1}(s) = \frac{P(s)}{Z(s)}.\begin{bmatrix} \hat{g}_{11}(s) & \hat{g}_{12}(s) & \dots & \hat{g}_{1n}(s) \\ \hat{g}_{21}(s) & \hat{g}_{22}(s) & \dots & \hat{g}_{2n}(s) \\ \vdots & \vdots & \ddots & \vdots \\ \hat{g}_{n1}(s) & \hat{g}_{n2}(s) & \dots & \hat{g}_{nn}(s) \end{bmatrix} \quad (27)$$

where $P(s)$ and $Z(s)$ are the pole and approximate zero polynomials of $G(s)$ respectively. Based on the existence of an RHP transmission zero in $G(s)$,

$$Z(s) = (-s+z)M(s) \quad (28)$$

where $M(s)$ has roots with negative real parts.

By substituting Eqs. (23) and (27) into Eq. (7), the initial controller matrix expression $C_{n\times n,n,init1}(s)$ can be computed by simple matrix multiplication. Further adjustments can then be made to the controller to first reduce irrational transfer function expressions using model reduction techniques and then remove RHP poles with RHP zeros.

Proposition 1: With reference to the adjoint matrix of Eq. (26), let the vectors $\boldsymbol{v_q}$ and $\hat{\boldsymbol{g}}_{\boldsymbol{n}}$ be n-sized vectors defined respectively by

$$\boldsymbol{v_q} = \begin{bmatrix} v_{1q} & v_{2q} & \dots & v_{nq} \end{bmatrix}^T \quad (29)$$

$$\hat{\boldsymbol{g}}_{\boldsymbol{n}} = \begin{bmatrix} \hat{g}_{1n} & \hat{g}_{2n} & \dots & \hat{g}_{nn} \end{bmatrix}^T \quad (30)$$

where

$$v_{\gamma q} = \hat{g}_{\gamma q}(s) + \hat{g}_{\gamma n}(s).\frac{s.a_{n,q}(s)}{(s+z)}; \quad \gamma = 1, \dots, n. \quad (31)$$

With a closed-loop transfer function matrix $H_{n\times n,n}$ given by Eq. (23) and the plant inverse $G^{-1}(s)$ given by Eq. (27), the internal model controller $C_{n\times n,n,init1}(s)$ can be computed according to Eq. (32), i.e.

$$C_{n\times n,n,init1}(s) = G^{-1}(s)H_{n\times n,n} \quad (32)$$

to yield

$C_{n\times n,n,init1}(s)$

$$= \frac{P(s)}{(-s+z)M(s)} \times \begin{bmatrix} \boldsymbol{v_1}F_1 & \boldsymbol{v_2}F_2 & \dots & \boldsymbol{v_{n-1}}F_{n-1} & \hat{\mathbf{g}}_{\boldsymbol{n}}\mathrm{Fm}_n \end{bmatrix} \quad (33)$$

where

$$F_q = \frac{e^{-\theta_q s}}{\tau_q s+1}; \quad q = 1, \dots, n-1 \quad (34)$$

$$\mathrm{Fm}_n = \frac{-s+z}{s+z}.\frac{e^{-\theta_n s}}{\tau_n s+1}. \quad (35)$$

Proof: The proof is given in Appendix A1.

Remark 1: With appropriate steps taken to remove the right-half-plane poles with right-half-plane zeros in the controller matrix arising from the utilization of Proposition 1, the controller that emerges guarantees closed-loop stability as well as null steady-state offset for all outputs.

Remark 2: Eq. (33) will only be stable if each of $v_{\gamma q}(s)$ has the expression $(-s+z)$ as one of its factors. Theorem 1 will help us ensure that this condition is satisfied.

Theorem 1: For an open-loop-stable, $n \times n$ system with delays and a single RHP transmission zero at $s = z$, the expression

$$v_{\gamma q}(s) = \hat{g}_{\gamma q} + \hat{g}_{\gamma n}\frac{s.a_{n,q}}{(s+z)}, \quad \gamma = 1, \dots, n; \quad q = 1, \dots, n-1 \quad (36)$$

has the expression $-s+z$ as one of its factors if and only if

$$a_{n,q} = -2\hat{\mathrm{g}}_{\gamma q}(z)/\hat{\mathrm{g}}_{\gamma n}(z); \ \gamma = 1, \dots, n. \quad (37)$$

Proof: For $(-s+z)$ to be a factor of $v_{\gamma q}(s)$, $v_{\gamma q}(z)$ must be 0:

$$v_{\gamma q}(z) = \hat{g}_{\gamma q}(z) + \hat{g}_{\gamma n}(z)\frac{z.a_{n,q}(z)}{(z+z)} = 0$$
$$\hat{g}_{\gamma n}(z).a_{n,q}(z) = -2\hat{g}_{\gamma q}(z)$$
$$a_{n,q}(z) = -2\hat{\mathrm{g}}_{\gamma q}(z)/\hat{\mathrm{g}}_{\gamma n}(z); \ \gamma = 1, \dots, n. \quad (38)$$

Remark 3: Based on Eq. (38), because each of $a_{n,q}(z)$ is unique for a particular value of n and q, then

$$\hat{\mathrm{g}}_{1q}(z)/\hat{\mathrm{g}}_{1n}(z) = \hat{\mathrm{g}}_{2q}(z)/\hat{\mathrm{g}}_{2n}(z) = \dots = \hat{\mathrm{g}}_{nq}(z)/\hat{\mathrm{g}}_{nn}(z). \quad (39)$$

Eq. (39) holds for every square matrix with an RHP transmission zero at $s = z$ and an adjoint matrix of Eq. (26).

Remark 4: As shown in Theorem 2 (Section III-B), a procedure similar to that of the proof of Theorem 1 can be used to develop conditions to actualize a triangular decoupling IMC design that moves inverse responses and control-loop interactions to the ith output ($i < n$).

With $M_{n,\gamma q}$ defined as

$$M_{n,\gamma q} = \left(\hat{\mathrm{g}}_{\gamma q}(s) + \hat{\mathrm{g}}_{\gamma n}(s).\frac{s.a_{n,q}(s)}{(s+z)}\right) \Big/ (-s+z) \quad (40)$$

substitution of Eq. (40) into Eq. (33), with the RHP zero and pole terms removed, leads to the final internal model controller achieving shifting of inverse responses and control-loop interactions to the nth output as

$$C_{n\times n,n,fin}(s) = \begin{bmatrix} \boldsymbol{c_1}F_1 & \boldsymbol{c_2}F_2 & \dots & \boldsymbol{c_{n-1}}F_{n-1} & \hat{\mathbf{g}}_{\boldsymbol{n}}\mathrm{ct}_n \end{bmatrix} \quad (41)$$

where F_q is as given in Eq. (34), $\hat{\mathbf{g}}_{\boldsymbol{n}}$ is as given in Eq. (30), and

$$\left.\begin{aligned} \boldsymbol{c_q} &= \begin{bmatrix} c_{1q} & c_{2q} & \dots & c_{nq} \end{bmatrix}^T; q = 1, \dots, n-1 \\ c_{\gamma q} &= \frac{P(s)M_{n,\gamma q}(s)}{M(s)}; \gamma = 1, \dots, n; q = 1, \dots, n-1 \\ \mathrm{ct}_n &= \frac{P(s)(s)e^{-\theta_n s}}{(s+z)M(s)(\tau_n s+1)} \end{aligned}\right\}. \quad (42)$$

B. ATDIMC SHIFTING INVERSE RESPONSES AND CONTROL-LOOP INTERACTIONS TO iTH OUTPUT FOR n × n SYSTEMS WITH DELAYS AND RHP TRANSMISSION ZEROS

Using Eqs. (19)-(22), for triangular decoupling to be achieved such that interactions and inverse responses are shifted to y_i ($i < n$), the closed-loop transfer function matrix $H_{n\times n,i}(s)$ can be written in block matrix form as,

$$H_{n\times n,i}(s) = \begin{bmatrix} H_{diag1,i} & 0_{(i-1)\times 1} & 0_{(i-1)\times(n-i)} \\ H_{row1,i} & H_{ii} & H_{row2,i} \\ 0_{(n-i)\times(i-1)} & 0_{(n-i)\times 1} & H_{diag2,i} \end{bmatrix} \quad (43)$$

where

$$\left.\begin{aligned} H_{diag1,i} &= diag\left\{H_{11}, H_{22}, \dots, H_{i-1,i-1}\right\} \\ H_{row1,i} &= \begin{bmatrix} H_{i1} & H_{i2} & \cdots & H_{i,i-1} \end{bmatrix} \\ H_{row2,i} &= \begin{bmatrix} H_{i,i+1} & H_{i,i+2} & \cdots & H_{in} \end{bmatrix} \\ H_{diag2,i} &= diag\left\{H_{i+1,i+1}, H_{i+2,i+2}, \dots, H_{nn}\right\} \end{aligned}\right\} \quad (44)$$

and $0_{(i-1)\times 1}$, $0_{(i-1)\times(n-i)}$, $0_{(n-i)\times(i-1)}$ and $0_{(n-i)\times 1}$ are, respectively, $(i-1)\times 1$, $(i-1)\times(n-i)$, $(n-i)\times(i-1)$ and $(n-i)\times 1$ zero matrices. In Eq. (44),

$$\left.\begin{aligned} H_{kk} &= \frac{e^{-\theta_k s}}{\tau_k s+1}; k = 1, \dots, i-1, i+1, \dots, n \\ H_{ir} &= \frac{s.a_{i,r}}{(s+z)}.\frac{e^{-\theta_r s}}{\tau_r s+1}; r = 1, \dots, i-1, i+1, \dots, n \\ H_{ii} &= \frac{-s+z}{s+z}.\frac{e^{-\theta_i s}}{\tau_i s+1} \end{aligned}\right\} \quad (45)$$

with $a_{i,r}$ being a constant whose value is to be determined. The procedure for determining $a_{i,r}$ is discussed in Theorem 2 and is similar to that of $a_{n,q}$ in Theorem 1.

As indicated in Section II-B, the matrix in Eq. (43) is not technically triangular but becomes triangular by rearranging the vectors that are related by the matrix. Thus, if

$$\boldsymbol{Y_{n\times n,i}}(s) = H_{n\times n,i}(s)\,\boldsymbol{R_{n\times n,i}}(s) \quad (46)$$

where

$$\boldsymbol{Y_{n\times n,i}}(s) = \begin{bmatrix} Y_1(s) & Y_2(s) & \dots & Y_n(s) \end{bmatrix}^T \quad (47)$$

$$\boldsymbol{R_{n\times n,i}}(s) = \begin{bmatrix} R_1(s) & R_2(s) & \dots & R_n(s) \end{bmatrix}^T \quad (48)$$

then, by rearranging the elements of the vectors in Eqs. (47) and (48) such that

$\boldsymbol{Y_{n\times n,i,2}}(s)$

$$= \left[Y_1(s) \quad \ldots \quad Y_{i-1}(s) \quad Y_{i+1}(s) \quad \ldots \quad Y_n(s) \quad Y_i(s) \right]^T \quad (49)$$

$$\boldsymbol{R_{n\times n,i,2}}(s) = \left[R_1(s) \quad \ldots \quad R_{i-1}(s) \quad R_{i+1}(s) \quad \ldots \quad R_n(s) \quad R_i(s) \right]^T \quad (50)$$

Eq. (46) becomes

$$\boldsymbol{Y_{n\times n,i,2}}(s) = H_{n\times n,i,2}(s)\, \boldsymbol{R_{n\times n,i,2}}(s) \quad (51)$$

where $H_{n\times n,i,2}(s)$ is given by

$$H_{n\times n,i,2}(s) = \begin{bmatrix} H_{diag1,i} & 0_{(i-1)\times 1} & 0_{(i-1)\times(n-i)} \\ 0_{(n-i)\times(i-1)} & H_{diag2,i} & 0_{(n-i)\times 1} \\ H_{row1,i} & H_{row2,i} & H_{ii} \end{bmatrix} \quad (52)$$

and the sub-matrices of $H_{n\times n,i,2}(s)$ are the same as in Eq. (44).

It is easy to see that $H_{n\times n,i,2}(s)$ can easily be derived from $H_{n\times n,i}(s)$. It is also easy to see that $H_{n\times n,i,2}(s)$ is of the same triangular form as $H_{n\times n,n}(s)$ of Eq. (23). The matrix of Eq. (45) can therefore be recast into the form of Eq. (52) and used to design a triangular decoupling internal model controller that shifts inverse responses and interactions to the ith output ($i < n$) using a procedure similar to that in Section III-A.

Proposition 2: With reference to the adjoint matrix of Eq. (26), let the vectors $\boldsymbol{v_r}$ and $\hat{\mathbf{g}}_{\boldsymbol{i}}$ be n-sized vectors defined respectively by

$$\boldsymbol{v_r} = \left[v_{1r} \quad v_{2r} \quad \ldots \quad v_{nr} \right]^T \quad (53)$$

$$\hat{\mathbf{g}}_{\boldsymbol{i}} = \left[\hat{\mathrm{g}}_{1i} \quad \hat{\mathrm{g}}_{2i} \quad \cdots \quad \hat{\mathrm{g}}_{ni} \right]^T \quad (54)$$

where

$$v_{wr} = \hat{\mathrm{g}}_{wr}(s) + \hat{\mathrm{g}}_{wi}(s).\frac{s.a_{i,q}(s)}{(s+z)}; \quad w = 1, 2, \ldots, n; \quad r = 1, \ldots, i-1,\ i+1, \ldots, n. \quad (55)$$

With a closed-loop transfer function matrix $H_{n\times n,i}$ given by Eq. (43) and the plant inverse $G^{-1}(s)$ given by Eq. (27), the internal model controller $C_{n\times n,i,init1}(s)$ can be computed according to

$$C_{n\times n,i,init1}(s) = G^{-1}(s) H_{n\times n,i} \quad (56)$$

to yield

$$C_{n\times n,i,init1}(s) = \frac{P(s)}{(-s+z)\,M(s)} \times \left[\boldsymbol{v_1}F_1 \quad \ldots \quad \boldsymbol{v_{i-1}}F_{i-1} \quad \boldsymbol{v_{i+1}}F_{i+1} \quad \cdots \quad \boldsymbol{v_n}F_n \quad \hat{\mathbf{g}}_{\boldsymbol{i}}\mathrm{Fm}_i \right] \quad (57)$$

where

$$F_q = \frac{e^{-\theta_q s}}{\tau_q s + 1}; \quad q = 1, \ldots, i-1,\ i+1, \ldots, n \quad (58)$$

$$\mathrm{Fm}_i = \frac{-s+z}{s+z}.\frac{e^{-\theta_i s}}{\tau_i s + 1}. \quad (59)$$

Proof: The proof is given in Appendix A2.

Remark 5: With appropriate steps taken to remove the right-half-plane poles with right-half-plane zeros in the controller matrix arising from the utilization of Proposition 2, the controller that emerges guarantees closed-loop stability as well as null steady-state offset for all outputs.

Remark 6: Eq. (57) will be stable only if $v_{wr}(s)$ in Eq. (55) has the expression $(-s+z)$ as one of its factors. Theorem 2 will help us ensure that this condition is satisfied.

Theorem 2: For an open-loop-stable, $n \times n$ system with delays and a single RHP transmission zero at $s = z$, the expression

$$v_{wr}(s) = \hat{\mathrm{g}}_{wr}(s) + \hat{\mathrm{g}}_{wi}(s).\frac{s.a_{i,r}(s)}{s+z}, w = 1, 2, \ldots, n; \quad r = 1 \ldots, i-1, i+1, \ldots, n \quad (60)$$

has the expression $-s+z$ as one of its factors if and only if

$$a_{i,r} = -2\hat{\mathrm{g}}_{wr}(z)\big/\hat{\mathrm{g}}_{wi}(z); \quad w = 1, \ldots, n. \quad (61)$$

Proof: For $(-s+z)$ to be a factor of $v_{wr}(s)$, $v_{wr}(z)$ must be 0, i.e.,

$$\begin{aligned} v_{wr}(z) &= \hat{\mathrm{g}}_{wr}(z) + \hat{\mathrm{g}}_{wi}(z).\frac{z.a_{i,r}(z)}{(z+z)} = 0 \\ \hat{\mathrm{g}}_{wi}(z).a_{i,r}(z) &= -2\hat{\mathrm{g}}_{wr}(z) \\ a_{i,r}(z) &= -2\hat{\mathrm{g}}_{wr}(z)\big/\hat{\mathrm{g}}_{wi}(z); \quad w = 1, \ldots, n. \end{aligned} \quad (62)$$

Remark 7: Based on Eq. (62), since each of $a_{i,r}(z)$ is unique for a particular value of i and r, then

$$\hat{\mathrm{g}}_{1r}(z)\big/\hat{\mathrm{g}}_{1i}(z) = \hat{\mathrm{g}}_{2r}(z)\big/\hat{\mathrm{g}}_{2i}(z) = \ldots = \hat{\mathrm{g}}_{nr}(z)\big/\hat{\mathrm{g}}_{ni}(z). \quad (63)$$

As in Eq. (39), Eq. (63) holds for every square matrix with an RHP transmission zero at $s = z$ and an adjoint of Eq. (26).

With $M_{i,wr}$ defined as

$$M_{i,wr} = \left(\hat{\mathrm{g}}_{wr}(s) + \hat{\mathrm{g}}_{wi}(s).\frac{s.a_{i,q}(s)}{(s+z)} \right) \Big/ (-s+z) \quad (64)$$

the appropriate substitutions and the removal of the RHP pole and zero terms lead to the final internal model controller achieving shifting of inverse responses and control-loop interactions to the ith output as

$$C_{n\times n,i,fin}(s) = \left[\boldsymbol{c_1}F_1 \quad \ldots \quad \boldsymbol{c_{i-1}}F_{i-1} \quad \boldsymbol{c_{i+1}}F_{i+1} \quad \cdots \quad \boldsymbol{c_n}F_n \quad \hat{\mathrm{g}}_{\boldsymbol{i}}\mathrm{ct}_i \right] \quad (65)$$

where F_r is as given in Eq. (58), $\hat{\mathrm{g}}_n$ as given in Eq. (54), and $\boldsymbol{c_r}$, c_{wr} and ct_i are as given in Eq. (66).

$$\left.\begin{aligned} \boldsymbol{c_r} &= \left[c_{1r} \ c_{2r} \ \ldots \ c_{nr} \right]^T; \\ & r = 1, 2, \ldots, i-1, i+1, \ldots, n \\ c_{wr} &= \frac{P(s)M_{i,wr}(s)}{M(s)}; w = 1, \ldots, n; \\ & r = 1, 2, \ldots, i-1, i+1, \ldots, n \\ \mathrm{ct}_i &= \frac{P(s)e^{-\theta_i s}}{(s+z)M(s)(\tau_i s+1)} \end{aligned}\right\}. \quad (66)$$

C. MODIFIED ATDIMC FOR MITIGATION OF SEVERE INTERACTION EFFECTS ON LEAST-DESIRED OUTPUT y_n

For some systems with strong couplings between control loops, at least one of the n ATDIMC designs has its least-desired output experiencing severe interaction effect from another output strongly coupled to it originally, potentially causing the overall error-index value to increase significantly in comparison with that of the dynamic decoupling IMC design.

To mitigate the effect of this strong interaction, a modified ATDIMC scheme is proposed which replaces the interaction expression in the closed-loop transfer function matrix with an all-pass expression in the diagonal element corresponding to the output strongly coupled to the least-desired output. This essentially nullifies the strong interaction effect from y_n and replaces it with an inverse response in the other output $y_j (j < n)$ that was strongly coupled to y_n in the first place.

Mathematically, let the expression "imperfect $y_j\&y_n$" describe an ATDIMC design that modifies the ATDIMC design of Section III-A such that the effect of the interaction between outputs y_j and y_n is removed from imperfect output y_n, with an inverse response then introduced to y_j. This modification yields 2 least-desired outputs y_j and y_n, with y_j having only an inverse response and y_n having a combination of an inverse response and $n-2$ control-loop-interaction features as a result of couplings between y_n and other outputs aside y_j, i.e. $y_1, y_2, \ldots, y_{j-1}, y_{j+1}, \ldots, y_{n-1}$.

The emerging closed-loop transfer function $H_{n\times n,y_jy_n}$ becomes a modified version of Eq. (23), i.e.

$$H_{n\times n,y_jy_n}(s) = \begin{bmatrix} H_{diag1,y_jy_n} & 0_{(j-1)\times 1} & 0_{(j-1)\times(n-j-1)} & 0_{(j-1)\times 1} \\ 0_{1\times(j-1)} & H_{jj} & 0_{1\times(n-j-1)} & 0 \\ 0_{(n-j-1)\times(j-1)} & 0_{(n-j-1)\times 1} & H_{diag2,y_jy_n} & 0_{(n-j-1)\times 1} \\ H_{row1,y_jy_n} & 0 & H_{row2,y_jy_n} & H_{nn} \end{bmatrix}, \tag{67}$$

where

$$\left.\begin{aligned} H_{diag1,y_jy_n} &= diag\left\{H_{11}, H_{22}, \ldots, H_{j-1,j-1}\right\} \\ H_{diag2,y_jy_n} &= diag\left\{H_{j+1,j+1}, \ldots, H_{n-1,n-1}\right\} \\ H_{row1,y_jy_n} &= \begin{bmatrix} H_{n1} & H_{n2} & \cdots & H_{n,j-1} \end{bmatrix} \\ H_{row2,y_jy_n} &= \begin{bmatrix} H_{n,j+1} & H_{n,j+2} & \cdots & H_{n,n-1} \end{bmatrix} \end{aligned}\right\}. \tag{68}$$

As evident, Eq. (23) for the "imperfect y_n" ATDIMC design has been modified to Eq. (67) for the "imperfect $y_j\&y_n$" ATDIMC design. It is noteworthy that both H_{jj} and H_{nn} are lone non-zero elements of the jth and nth columns of $H_{n\times n,y_jy_n}$(s) respectively.

For Eq. (68),

$$\left.\begin{aligned} H_{kk} &= \frac{e^{-\theta_k s}}{\tau_k s+1}; k = 1, \ldots, j-1, j+1, \ldots, n-1; \\ H_{jj} &= \frac{-s+z}{s+z}.\frac{e^{-\theta_j s}}{\tau_j s+1} \\ H_{np} &= \frac{s.a_{n,p}(s)}{(s+z)}.\frac{e^{-\theta_p s}}{\tau_p s+1}; \\ p &= 1, \ldots, j-1, j+1, \ldots, n-1; H_{nj} = 0 \\ H_{nn} &= \frac{-s+z}{s+z}.\frac{e^{-\theta_n s}}{\tau_n s+1} \end{aligned}\right\}. \tag{69}$$

As with previous designs, the initial controller $C_{n\times n,jn,init1}(s)$ can be described by modified versions in Eqs. (33) to (35), leading to

$$\begin{aligned} &C_{n\times n,jn,init1}(s) \\ &= \frac{P(s)}{(-s+z)M(s)} \\ &\quad\times\left[\boldsymbol{v_1}F_1 \quad \ldots \quad \boldsymbol{v_{j-1}}F_{j-1} \quad \hat{\mathbf{g}}_{\boldsymbol{i}}\mathrm{Fm}_i \quad \boldsymbol{v_{j+1}}F_{j+1} \quad \cdots \right. \\ &\qquad \left. \boldsymbol{v_{n-1}}F_{n-1} \quad \hat{\mathbf{g}}_{\boldsymbol{n}}\mathrm{Fm}_n\right], \end{aligned} \tag{70}$$

where

$$\left.\begin{aligned} \boldsymbol{v_q} &= \begin{bmatrix} v_{1q} & v_{2q} & \ldots & v_{nq} \end{bmatrix}^T; \\ q &= 1, \ldots, j-1, j+1, \ldots, n-1 \\ F_q &= \frac{e^{-\theta_q s}}{\tau_q s+1}; q = 1, \ldots, j-1, j+1, \ldots, n-1 \\ \hat{\mathbf{g}}_{\boldsymbol{\alpha}} &= \begin{bmatrix} \hat{\mathrm{g}}_{1\alpha} & \hat{\mathrm{g}}_{2\alpha} & \ldots & \hat{\mathrm{g}}_{n\alpha} \end{bmatrix}^T; \alpha = j, n \\ \mathrm{Fm}_\alpha &= \frac{-s+z}{s+z}.\frac{e^{-\theta_\alpha s}}{\tau_\alpha s+1}; \alpha = j, n \end{aligned}\right\} \tag{71}$$

and $v_{\boldsymbol{\gamma}q}$ is as given in Eq. (31) for $\gamma = 1, \ldots, n; q = 1, \ldots, j-1, j+1, \ldots, n-1$.

Using the procedure in Section III-A for developing the controller transfer function matrix, the internal model controller that achieves "imperfect y_j and y_n" such that the effect of the interaction between outputs y_j and y_n is removed from imperfect output y_n, with an inverse response then introduced to y_j, is given by

$$\begin{aligned} &C_{n\times n,jn,fin}(s) \\ &= \left[\boldsymbol{c_1}F_1 \quad \ldots \quad \boldsymbol{c_{j-1}}F_{j-1} \quad \hat{\mathrm{g}}_i\mathrm{ct}_i \quad \boldsymbol{c_{j+1}}F_{j+1} \quad \cdots \right. \\ &\qquad \left. \boldsymbol{c_{n-1}}F_{n-1} \quad \hat{\mathbf{g}}_{\boldsymbol{n}}\mathrm{ct}_n\right] \end{aligned} \tag{72}$$

where F_q is as given in the 2nd sub-equation of Eq. (71), $\hat{\mathbf{g}}_{\boldsymbol{\alpha}}$ is as given in the 3rd sub-equation of Eq. (71), and

$$\left.\begin{aligned} \boldsymbol{c_q} &= \begin{bmatrix} c_{1q} & c_{2q} & \ldots & c_{nq} \end{bmatrix}^T; \\ q &= 1, \ldots, j-1, j+1, \ldots, n-1 \\ \mathrm{ct}_\alpha &= \frac{P(s)e^{-\theta_\alpha s}}{(s+z)M(s)(\tau_\alpha s+1)}; \alpha = j, n \end{aligned}\right\}. \tag{73}$$

D. MODIFIED ATDIMC FOR MITIGATION OF SEVERE INTERACTION EFFECTS ON LEAST-DESIRED OUTPUT y_j

Similar to Section III-C above, let the expression "imperfect $y_j\&y_i$" describe an ATDIMC design that modifies the ATDIMC design of Section III-B such that the effect of

the interaction between outputs y_j and y_i is removed from imperfect output y_i, with an inverse response then introduced to y_j. This modification yields 2 least-desired outputs y_j and y_i, with y_j having only an inverse response and y_i having a combination of an inverse response and $n-2$ control-loop-interaction features as a result of couplings between y_i and other outputs aside y_j, i.e. $y_1, y_2, \ldots, y_{j-1}, y_{j+1}, y_{j+2} \ldots, y_{i-1}, y_{i+1}, y_{i+2}, \ldots, y_n$.

The emerging closed-loop transfer function $H_{n\times n,y_jy_i}$ becomes a modified version of Eq. (43), i.e., (74), as shown at the bottom of the page, where

$$\left.\begin{array}{r} H_{diag1,y_jy_n} = diag\left\{H_{11}, H_{22}, \ldots, H_{j-1,j-1}\right\} \\ H_{diag2,y_jy_n} = diag\left\{H_{j+1,j+1}, \ldots, H_{i-1,i-1}\right\} \\ H_{diag3,y_jy_n} = diag\left\{H_{i+1,i+1}, \ldots, H_{nn}\right\} \\ H_{row1,y_jy_n} = \begin{bmatrix} H_{n1} & H_{n2} & \cdots & H_{n,j-1} \end{bmatrix} \\ H_{row2,y_jy_n} = \begin{bmatrix} H_{n,j+1} & H_{n,j+2} & \cdots & H_{n,i-1} \end{bmatrix} \\ H_{row3,y_jy_n} = \begin{bmatrix} H_{n,i+1} & H_{n,i+2} & \cdots & H_{nn} \end{bmatrix} \end{array}\right\} \quad (75)$$

and

$$\left.\begin{array}{r} H_{kk} = \dfrac{e^{-\theta_k s}}{\tau_k s+1}; \\ k = 1, \ldots, j-1, j+1, \ldots, i-1, i+1, \ldots, n \\ H_{jj} = \dfrac{-s+z}{s+z}.\dfrac{e^{-\theta_j s}}{\tau_j s+1} \\ H_{ir} = \dfrac{s.a_{i,r}(s)}{(s+z)}.\dfrac{e^{-\theta_r s}}{\tau_r s+1}; \\ r = 1, \ldots, j-1, j+1, \ldots, i-1, i+1, \ldots, n \\ H_{ii} = \dfrac{-s+z}{s+z}.\dfrac{e^{-\theta_i s}}{\tau_i s+1} \end{array}\right\}. \quad (76)$$

It is noteworthy that both H_{jj} and H_{ii} in Eq. (58) are the lone non-zero elements of the jth and ith columns of $H_{n\times n,y_jy_i}(s)$ respectively.

The initial controller $C_{n\times n,ji,init1}(s)$ that emerged using Eq. (5) can be described by modified versions in Eqs. (53)-(59), i.e.

$$\begin{aligned} &C_{n\times n,ji,init1}(s) \\ &= \frac{P(s)}{(-s+z)M(s)} \\ &\times\left[\boldsymbol{v_1}F_1 \quad \ldots \quad \boldsymbol{v_{j-1}}F_{j-1} \quad \hat{\mathrm{g}}_j Fm_j \quad \boldsymbol{v_{j+1}}F_{j+1} \quad \cdots \right. \\ &\quad \left. \boldsymbol{v_{i-1}}F_{i-1} \quad \hat{\mathrm{g}}_i \mathrm{Fm_i} \quad \boldsymbol{v_{i+1}}F_{i+1} \quad \cdots \quad \boldsymbol{v_n}F_n\right] \end{aligned} \quad (77)$$

where

$$\left.\begin{array}{r} \boldsymbol{v_r} = \begin{bmatrix} v_{1r} & v_{2r} & \ldots & v_{nr} \end{bmatrix}^T \\ F_r = \dfrac{e^{-\theta_r s}}{\tau_r s+1} \\ \hat{\mathbf{g}}_{\boldsymbol{\alpha}} = \begin{bmatrix} \hat{\mathrm{g}}_{1\alpha} & \hat{\mathrm{g}}_{2\alpha} & \cdots & \hat{\mathrm{g}}_{n\alpha} \end{bmatrix}^T; \alpha = j, i \\ Fm_\alpha = \dfrac{-s+z}{s+z}.\dfrac{e^{-\theta_\alpha s}}{\tau_\alpha s+1}; \alpha = j, i \end{array}\right\}. \quad (78)$$

For the 1st and 2nd sub-equations of Eq. (78), r takes values $1, 2, \ldots, j-1, j+1, \ldots, i-1, i+1, \ldots, n$.

Using the procedure in Section III-B to develop the controller yields the internal model controller achieving imperfect y_j and y_i as

$$\begin{aligned} &C_{n\times n,ji,fin}(s) \\ &= \left[\boldsymbol{c_1}F_1 \quad \ldots \quad \boldsymbol{c_{j-1}}F_{j-1} \quad \hat{\mathrm{g}}_j ct_j \quad \boldsymbol{c_{j+1}}F_{j+1} \quad \cdots \right. \\ &\quad \left. \boldsymbol{c_{i-1}}F_{i-1} \quad \hat{\mathrm{g}}_i \mathrm{ct_i} \quad \boldsymbol{c_{i+1}}F_{i+1} \quad \cdots \quad \boldsymbol{c_n}F_n\right] \end{aligned} \quad (79)$$

where F_q is as given in the 2nd sub-equation of Eq. (78), $\hat{\mathbf{g}}_{\boldsymbol{\alpha}}$ is as given in the 3rd sub-equation of Eq. (78), and

$$\left.\begin{array}{r} \boldsymbol{c_r} = \begin{bmatrix} c_{1r} & c_{2r} & \ldots & c_{nr} \end{bmatrix}^T \\ c_{wr} = \dfrac{P(s)M_{i,wr}(s)}{M(s)}; w = 1, \ldots, n \\ \mathrm{ct}_\alpha = \dfrac{P(s)e^{-\theta_\alpha s}}{(s+z)M(s)(\tau_\alpha s+1)}; \alpha = j, i \end{array}\right\}. \quad (80)$$

Remark 8: It is technically possible to eliminate more than one interaction effect if there are multiple severe interaction effects on the least-desired outputs of Sections III-A and III-B, since the closed-loop transfer function matrix remains triangular. However, the advantage of using the ATDIMC may be lost if multiple interaction effects are replaced by inverse responses on the outputs coupled to the least-important output; hence, the decision to limit the removed interaction effect to just one. In fact, the limiting situation that results from replacing all interactions with the corresponding inverse responses on the outputs coupled to the least-important output is equivalent to dynamic decoupling.

IV. MODEL SIMPLIFICATION FOR ELEMENTS OF THE CONTROLLER TRANSFER FUNCTION MATRIX

As previously shown, for the designs of Sections III-A and III-B, the expressions $M_{n,\gamma q}(s)$ and $M_{i,wr}(s)$ are developed according to Eqs. (40) and (64) respectively, with the same expressions then used respectively in Sections III-C and III-D for the modified ATDIMC designs. According to Eqs. (40) and (64), both $M_{n,\gamma q}(s)$ and $M_{i,wr}(s)$ are developed using the appropriate elements of the adjoint

$$H_{n\times n,y_jy_i} = \begin{bmatrix} H_{diag1,y_jy_i} & 0_{(j-1)\times 1} & 0_{(j-1)\times(i-j-1)} & 0_{(j-1)\times 1} & 0_{(j-1)\times(n-i)} \\ 0_{1\times(j-1)} & H_{jj} & 0_{1\times(i-j-1)} & 0 & 0_{1\times(n-i)} \\ 0_{(i-j-1)\times(j-1)} & 0_{(i-j-1)\times 1} & H_{diag2,y_jy_i} & 0_{(i-j-1)\times 1} & 0_{(i-j-1)\times(n-i)} \\ H_{row1,y_jy_n} & 0 & H_{row2,y_jy_n} & H_{ii} & H_{row3,y_jy_n} \\ 0_{(n-i)\times(j-1)} & 0_{(n-i)\times 1} & 0_{(n-i)\times(i-j-1)} & 0_{(n-i)\times 1} & H_{diag3,y_jy_i} \end{bmatrix} \quad (74)$$

of the transfer function matrix of the plant. Because adjoints of the transfer function matrices of systems with delays have irrational elements for $n > 2$, $M_{n,\gamma q}(s)$ and $M_{i,wr}(s)$ are irrational. Because both $M_{n,\gamma q}(s)$ and $M_{i,wr}(s)$ are used to develop the transfer function matrices of the controllers for all designs, some model simplification is necessary to reduce $M_{n,\gamma q}(s)$ and $M_{i,wr}(s)$ to rational-transfer-function-plus-delay expressions $\hat{M}_{n,\gamma q}(s)$ and $\hat{M}_{i,wr}(s)$ such that

$$\hat{M}_{n,\gamma q}(s) = \hat{M}_{rat,n,\gamma q}(s)\, e^{-d_{n,\gamma q}s} \tag{81}$$

$$\hat{M}_{i,wr}(s) = \hat{M}_{rat,i,wr}(s)\, e^{-d_{i,wr}s} \tag{82}$$

where $\hat{M}_{rat,n,\gamma q}$ and $\hat{M}_{rat,i,wr}$ are rational and proper transfer functions, and $d_{n,\gamma q}$ and $d_{n,\gamma q}$ are real and positive numbers.

Similarly, the adjoint elements $\hat{g}_{\gamma n}(s)$ and $\hat{g}_{wr}(s)$, directly used in the controller matrix development in Sections III-A and III-C (2nd sub-equation of Eqs. (42) and 3rd sub-equation of Eq. (71)), and III-B and III-D (Eqs. (55) and the 3rd sub-equation of Eq. (78)), are irrational for $n \times n$ systems ($n > 2$) and require some model simplification to rational-transfer-function-plus-delay expressions $\tilde{\hat{g}}_{\gamma n}$ and $\tilde{\hat{g}}_{wr}$ such that

$$\tilde{\hat{g}}_{\gamma n}(s) = \tilde{\hat{g}}_{rat,\gamma n}(s)\, e^{-d_{\gamma n}s} \tag{83}$$

$$\tilde{\hat{g}}_{wr}(s) = \tilde{\hat{g}}_{rat,wr}(s)\, e^{-d_{wr}s} \tag{84}$$

where $\tilde{\hat{g}}_{rat,\gamma n}$ and $\tilde{\hat{g}}_{rat,wr}$ are rational and proper transfer functions, and $d_{\gamma n}$ and d_{wr} are real and positive numbers.

The recursive least squares techniques of [39] were used in [11], [12], and [20] for appropriate reductions of controller terms, whereas moment matching was used in [14]. In this study, the method of model simplification used was the method of minimization of the Integral Time-Weighted Absolute Error (ITAE) of the difference between the step responses of the actual and reduced expressions. This provides a good opportunity for responses of original and reduced functions to be observed. The basic graphical knowledge of step responses to transfer functions of different orders is used to dictate transfer-function structures and constraints for the reductions.

Mathematically, for the irrational transfer function expression $\varphi(s)$, if the symbol "$\mathcal{L}^{-1}$" represents the Inverse Laplace Transform, then the unit step response can be written as

$$\varphi_{step,actual}(t) = \mathcal{L}^{-1}\left\{\frac{\varphi(s)}{s}\right\} \tag{85}$$

while for the reduced expression $\hat{\varphi}(s)$, given by

$$\begin{aligned}\hat{\varphi}(s) &= \frac{N(s)}{D(s)}e^{-ds} \\ &= \frac{\alpha_P s^p + \alpha_{P-1}s^{p-1} + \ldots + \alpha_2 s^2 + \alpha_1 s + 1}{\beta_q s^q + \beta_{q-1}s^{q-1} + \ldots + \beta_2 s^2 + \beta_1 s + 1}e^{-ds}\end{aligned} \tag{86}$$

the unit step response can be written as

$$\varphi_{step,reduced}(t) = L^{-1}\left\{\frac{\hat{\varphi}(s)}{s}\right\}. \tag{87}$$

The error e between the responses of the actual and reduced expressions is given by

$$e(t) = \varphi_{step,actual}(t) - \varphi_{step,reduced}(t) \tag{88}$$

and the ITAE is given by

$$ITAE = \int_{t_{init}}^{t_{final}} t\,|e(t)|dt. \tag{89}$$

The minimization of the ITAE can be performed using a host of optimization schemes provided in MATLAB/SIMULINK, with the common choices being Pattern Search and Genetic Algorithms.

It is noteworthy that for each of the regular ATDIMC designs for a system, a reduction must take place for each element of the transfer function matrix of the controller. This means that n^2 reductions are performed to get each of the n regular ATDIMC controllers. For one of the n regular ATDIMC designs, the computational complexity is comparable to that of simplified decoupling of [20] that performs reduction of all elements of an $n \times n$ decoupler and an apparent process. Also, just as techniques like simplified decoupling of [20] and inverted decoupling of [19] provide multiple options and configurations from which one makes the best choice, the n ATDIMC designs are possibilities from which the best can be selected based on control objectives.

V. ROBUSTNESS ANALYSIS OF ATDIMC DESIGNS

As pointed out in [16], for a square multivariable control system in the IMC configuration, if $G(s)$ is the plant being controlled, $C(s)$ is the controller in the IMC configuration, $K(s)$ is the conventional-feedback-controller equivalent to $C(s)$, $S(s)$ is the sensitivity function and $T_I(s)$ is the complementary sensitivity function, then if μ-analysis is performed on the designed control system, then robust stability and robust performance are both assured if both structured singular values μ_{RS} and μ_{RP} of robust stability and robust performance respectively are less than unity, i.e.,

$$\mu_{RS} = \mu\left[-W_I(s)T_I(s)\right] < 1 \tag{90}$$

$$\mu_{RP} = \mu\begin{bmatrix} -W_I(s)T_I(s) & -W_I(s)K(s)S(s) \\ W_P(s)S(s)G(s) & W_P(s)S(s) \end{bmatrix} < 1 \tag{91}$$

where W_I and W_P are both $n \times n$ diagonal matrices representing weights for multiplicative input uncertainty and performance at the output respectively, and are given by

$$W_I = diag\{w_i \quad w_i \quad \ldots \quad w_i\} \tag{92}$$

$$W_p = diag\{w_p \quad w_p \quad \ldots \quad w_p\}. \tag{93}$$

In Eq. (92), the uncertainty weight w_i is expressed as

$$w_i(s) = \frac{\tau s + r_0}{\left(\frac{\tau}{r_\infty}\right)s + 1} \tag{94}$$

where r_0 is the relative uncertainty at steady-state, $\frac{1}{\tau}$ is the approximate frequency at which the relative uncertainty reaches 100%, and r_∞ is the magnitude of the weight at high frequency.

In Eq. (93), the performance weight w_P is expressed as

$$w_P(s) = \frac{\frac{s}{M} + \omega_B^*}{s + \omega_B^* A} \tag{95}$$

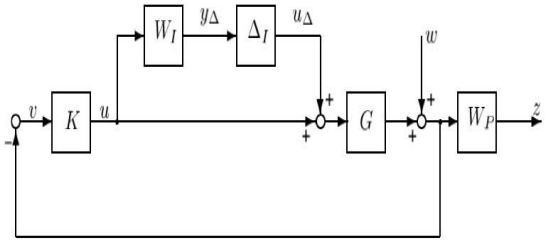

FIGURE 2. Block diagram for robust performance with multiplicative input uncertainty within conventional feedback configuration.

where M is the peak sensitivity (whose inverse is w_p at high frequencies), A is a parameter (whose inverse is w_p at low frequencies) and ω_B^* is the system bandwidth. Figure 2 shows a block diagram of the multiplicative input uncertainty and the performance uncertainty measured at the output.

In this study, μ-analysis was performed on each of the designed controllers to test for robust stability and robust performance. As will be seen, at least one ATDIMC design yields better robustness results than the dynamic decoupling counterpart, with the designs with severe interactions in the least-desired outputs expectedly yielding poor robust performance results. It will also be seen that the modified ATDIMC designs improve on the robustness results of the original ATDIMC designs being modified. The details of the chosen uncertainty and performance weights are provided in Section VI.

VI. SIMULATION RESULTS

A. THE 3 × 3 DEPROPANIZER

The Depropanizer, presented in literature as a control system that separates propane from the feed that comes from a deethanizer column in distillation control [6], has the following transfer function matrix:

$$G(s) = \begin{bmatrix} \frac{-0.2697}{97.5s+1}e^{-27.5s} & \frac{1.978}{118.5s+1}e^{-53.5s} & \frac{0.07724}{96s+1}e^{-56s} \\ \frac{0.4881}{56s+1}e^{-117s} & \frac{-5.26}{58.5s+1}e^{-26.5s} & \frac{0.19996}{51s+1}e^{-35s} \\ \frac{0.6}{40.5s+1}e^{-16.5s} & \frac{5.5}{19.5s+1}e^{-15.5s} & \frac{-0.5}{18s+1}e^{-17s} \end{bmatrix}. \tag{96}$$

This system has a dominant RHP transmission zero at $s = \mathbf{0.0120061}$. It also has strong couplings between the control loops, with the first channel interacting very strongly with the controls in the second and third channels.

Noting that n is 3 for this system, ATDIMC designs were made for the Depropanizer plant for "imperfect y_1" (Section III-B, $i = 1, n = 3$), "imperfect y_2" (Section III-B, $i = 2, n = 3$), "imperfect y_3" (Section III-A, $n = 3$), "imperfect y_1&y_2" (Section III-D, $j = 1, i = 2$), "imperfect y_1&y_3" (Section III-C, $j = 1, i = 3$) and "imperfect y_2&y_3" (Section III-C, $j = 2, i = 3$). The details of these designs are contained in Appendices B1 to B6 of this paper respectively.

For comparison, a dynamic decoupling IMC design was made using the method of [11], with implementations performed using the IMC structure and model reductions performed using the minimization of ITAE of step responses. In addition, the multivariable PID controllers in [20], achieved using simplified dynamic decoupling, were implemented and compared with the ATDIMC, modified ATDIMC, and dynamic decoupling IMC controllers in [18]. The details of the controllers in [18] and [20] are contained in Appendices B7 and B8 respectively.

With reference to Eqs. (94) and (95), the uncertainty and performance weights used in [20] were selected for the robustness analysis of the designed controllers. These weights are as presented in Eqs. (97) and (98).

$$w_{i,deprop}(s) = \frac{0.009s + 0.15}{0.0045s + 1} \tag{97}$$

$$w_{P,deprop}(s) = \frac{\frac{s}{2.75} + 0.00075}{s}. \tag{98}$$

The input uncertainty weight corresponds to approximately 15% uncertainty at low frequency and 200% uncertainty at high frequency, whereas the performance weight corresponds to integral action (for null steady-state error) and a maximum sensitivity peak of $M = 2.75$.

The best of the designed ATDIMC controllers (design for "imperfect y_1") is tuned to attain a slightly better robust performance than the MV-PID design in [20]. The resulting tuning parameters were $\tau_1 = \tau_2 = \tau_3 = 105$. These tuning parameters were then used for all other ATDIMC and dynamic DIMC designs to compare both the robustness characteristics and nominal quantitative plant output and plant input characteristics for the same specified speeds of responses. The graphs of all these designs were also plotted for a visual comparison of plant input and plant output responses. Figure 3 shows the plant output and input plots while Table 1 shows the computed integral-absolute-error (IAE), total-variation (TV), μ_{RS} and μ_{RP} values for the plant outputs and plant inputs, respectively, for all the designs.

$$G(s) = \begin{bmatrix} \frac{2e^{-69.1463s}}{1.5s+1} & \frac{3.5e^{-18.1317s}}{5s+1} & \frac{3.75e^{-27.4206s}}{5.5s+1} & \frac{1.25e^{-20.2779s}}{4s+1} \\ \frac{7.225e^{-32.8696s}}{3.235s+1} & \frac{-10e^{-25.1989s}}{7s+1} & \frac{6e^{-10.0481s}}{2s+1} & \frac{4e^{-10.0223s}}{2.22s+1} \\ \frac{8.4e^{-37.2156s}}{3.14s+1} & \frac{3.8e^{-13.8045s}}{9.35s+1} & \frac{4e^{-10.0147s}}{6.3s+1} & \frac{9e^{-33.418s}}{4.24s+1} \\ \frac{-3.45e^{-30.9474s}}{12s+1} & \frac{4.6e^{-46.2443s}}{15s+1} & \frac{7.5e^{-24.4816s}}{2.3s+1} & \frac{5.2e^{-45.0222s}}{8.9s+1} \end{bmatrix}. \tag{99}$$

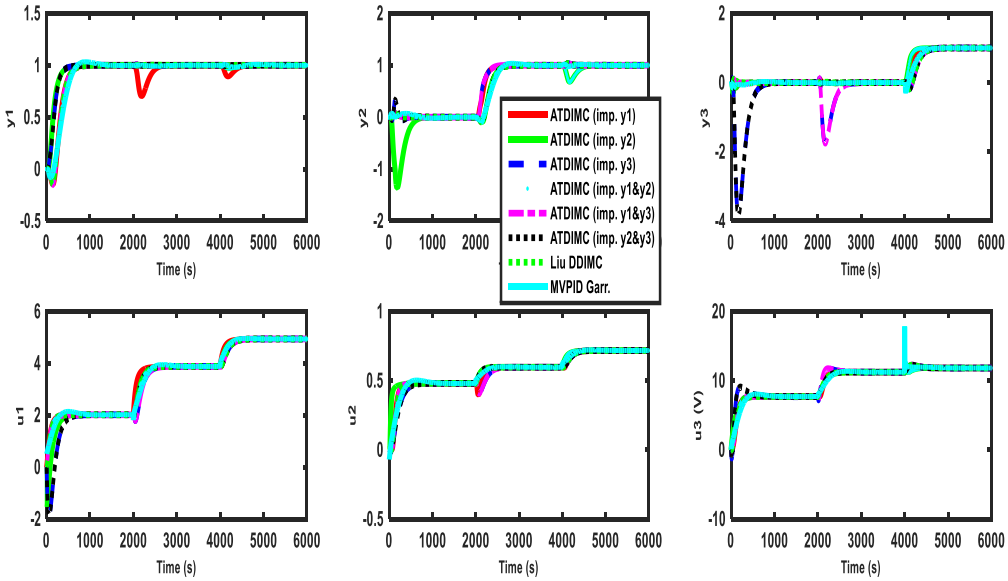

FIGURE 3. Plant output & input responses of ATDIMC, modified ATDIMC, dynamic DIMC and simplified decoupling schemes on 3 × 3 depropanizer, for tuning parameters $\tau_1 = \tau_2 = \tau_3 = 105$ and reference signals as unit step functions applied at 0s, 2000s and 4000s respectively.

TABLE 1. Comparison of performance indices of the ATDIMC and modified ATDIMC methods with dynamic DIMC methods for implementations on depropanizer, for tuning parameters as $\tau_1 = \tau_2 = \tau_3 = 105$.

Controller	IAE1	IAE2	IAE3	IAE TOTAL	TV1	TV2	TV3	TV TOTAL	μ_{RS}	μ_{RP}
ATDIMC (iy1)	476.8	201.1	203.9	881.8	3.464	0.8561	11.3	15.6201	0.1612	0.9968
ATDIMC (iy2)	187.6	792.4	136.9	1117	2.911	0.2494	4.757	7.9174	0.5374	1.8864
ATDIMC (iy3)	193.3	220.7	1824	2238	4.079	0.4416	9.251	13.7716	0.2150	2.5568
iy1y2	378.7	454.2	139.1	972	1.889	0.323	5.297	7.509	0.5374	1.8863
iy1y3	371	191.2	829.5	1392	2.246	0.3829	6.199	8.8279	0.2570	1.5064
iy2y3	191.9	404.3	1369	1965	4.681	0.4171	9.288	14.3861	0.2299	2.4540
DDIMC (Liu)	370	375.6	370	1116	2.049	0.3213	5.376	7.7463	0.1519	1.0978
MVPID (Garrido)	409.1	439.2	329.7	1178	2.955	0.4646	12.92	16.6	0.17	1.0000

TABLE 2. Comparison of performance indices of the ATDIMC and modified ATDIMC methods with dynamic DIMC methods for implementations on 4 × 4 F4d2 system, with tuning parameters as $\tau_1 = \tau_2 = \tau_3 = \tau_4 = 106$.

Controller	IAE1	IAE2	IAE3	IAE4	IAE TOTAL	TV1	TV2	TV3	TV4	TV TOT.	μ_{RS}	μ_{RP}
ATDIMC (iy1)	213.7	169.1	159.3	165.4	707.5	0.1146	0.09392	0.1506	0.1919	0.55102	0.1610	0.6858
ATDIMC (iy2)	148.4	493.3	126.5	173.4	941.5	0.1106	0.133	0.1604	0.1724	0.5764	0.1539	0.9903
ATDIMC (iy3)	151.6	146.7	333.5	162.2	793.9	0.08935	0.08335	0.1783	0.1903	0.5413	0.1519	0.7555
ATDIMC (iy4)	149.6	178.9	154.7	387.8	871	0.1715	0.1112	0.146	0.2143	0.643	0.1537	0.8312
iy1y2	176.3	338.1	120.9	151.6	786.9	0.1084	0.1519	0.1575	0.174	0.5918	0.1719	0.8026
iy3y2	146.4	407.5	184.1	173.2	911.2	0.1154	0.0904	0.1329	0.1558	0.4945	0.1587	0.9438
iy4y3	147.8	425.7	124	230.5	928.1	0.1091	0.1175	0.1748	0.1713	0.5727	0.1581	0.9446
DDIMC (Liu)	221	234.6	222.3	256.2	934.1	0.1588	0.1445	0.2038	0.2297	0.7368	0.1520	0.7695

B. THE 4 × 4 F4d2 SYSTEM OF [40]

The 4 × 4 F4d2 System of [40], with a dominant RHP zero at $s = 0.0432123$, has the transfer function matrix given as (99), shown at the bottom of the previous page.

This system has strong control-loop couplings, with the first channel interacting most strongly with the controls in the second, third and fourth channels.

Noting that n is 4 for this system, ATDIMC designs were made for the 4 × 4 F4d2 plant for "imperfect y_1" (Section III-B, $i = 1, n = 4$), "imperfect y_2" (Section III-B, $i = 2, n = 4$), "imperfect y_3" (Section III-B, $i = 3, n = 4$), "imperfect y_4" (Section III-A, $n = 4$), "imperfect y_1&y_2" (Section III-D, $j = 1, i = 2$), "imperfect y_3&y_2" (Section III-D, $j = 3, i = 2$) and "imperfect y_4&y_2" (Section III-D, $j = 4, i = 2$). The details of these designs are contained in Appendices C1 to C7 of this paper respectively. Several other modified ATDIMC designs could have been made but those made above were chosen because of the effect of the interaction component of the design for "imperfect y_2".

For comparison, a dynamic decoupling IMC design was done using the method in [18], with implementations performed using the IMC structure and model reductions

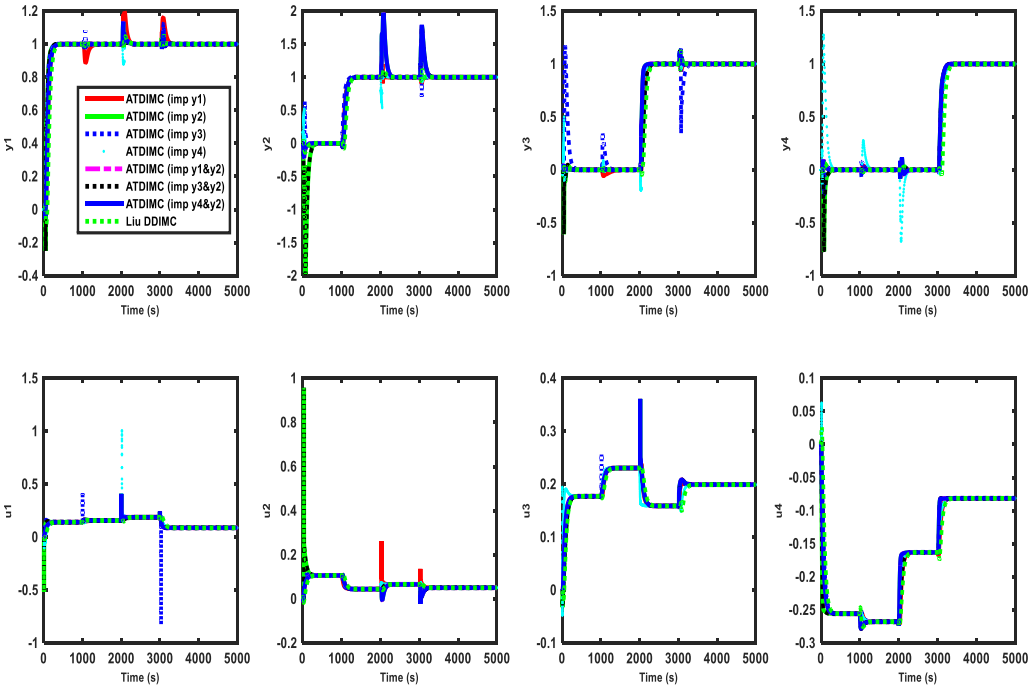

FIGURE 4. Plant output & input responses of ATDIMC, modified ATDIMC and dynamic DIMC schemes on 4 × 4 F4d2 system for $\tau_1 = \tau_2 = \tau_3 = \tau_4 = 106$, with reference signals as unit step functions applied at 0s, 1000s, 2000s and 3000s respectively.

performed using the minimization of the ITAE of step responses. This design was compared with the ATDIMC and modified ATDIMC designs. Details of the dynamic decoupling IMC design are provided in Appendix C8.

With reference to Eqs. (94) and (95), the uncertainty and performance weights chosen for the robustness analysis of the designed controllers are:

$$w_{i,F4d2}(s) = \frac{0.009s + 0.15}{0.0045s + 1} \tag{100}$$

$$w_{P,F4d2}(s) = \frac{\frac{s}{3.00} + 0.00075}{s}. \tag{101}$$

The input uncertainty weight corresponds to approximately 15% uncertainty at low frequency and 200% uncertainty at high frequency, whereas the performance weight corresponds to integral action (for null steady-state error) and a maximum sensitivity peak of $M = 3$.

The tuning parameters chosen for the designs are $\tau_1 = \tau_2 = \tau_3 = \tau_4 = 106$. These tuning parameters ensured a good trade-off between performance and robustness for the designed controllers. As in the case of the designs for the Depropanizer, robustness characteristics and nominal quantitative plant output and plant input characteristics were compared for the same specified speeds of responses. The graphs of all these designs are also plotted graphically for a visual comparison of plant input and plant output responses. Figure 4 shows the plant output and input response plots while Table 2 shows the computed IAE, TV, μ_{RS} and μ_{RP} values for the plant outputs and plant inputs respectively, for all the designs.

C. DISCUSSION OF RESULTS

From the plots and tables, it is seen that in each ATDIMC case for a single least-desired output, inverse responses and interactions are successfully transferred to the "imperfect output". For both systems, one ATDIMC design is guaranteed to have a lower overall output IAE value and higher robustness than the DIMC counterpart for the same tuning parameters, with at least one other ATDIMC design having a higher output IAE value and lower robustness than that of DIMC. Beyond IMC-based designs, it is fair to say based on the results of the designs on the 2 systems that the best ATDIMC design gives better nominal and robust results than the best dynamic decoupling design for a square stable multivariable system with delays and RHP transmission zeros, IMC-based or otherwise.

It is also possible that other ATDIMC and modified ATDIMC designs yield better nominal IAE values than those of dynamic decoupling IMC (as is the case for the F4d2 system that has three of the four ATDIMC designs and all three modified ATDIMC designs having lower IAE values than that of dynamic DIMC) and better robustness results (as is the case for the F4d2 system that has the design for "imperfect y_3" yielding marginally better robust stability and robust performance indices). However, superior nominal and robustness characteristics are guaranteed for a single ATDIMC design (the designs for "imperfect y_1" in both examples). This is consistent with the results obtained in [37] for the two-input, two-output case. If error indices and robustness are the principal considerations, the task is to determine which ATDIMC design yields the best nominal and robustness characteristics,

with the assurance that such a design will outperform existing frequency-domain-based dynamic decoupling designs with similar nominal and/or robustness specifications.

As shown in the plots and tables, in situations where the single least-desired output suffers from the effect of a severe interaction (as is the case for the ''imperfect y_2'' and ''imperfect y_3'' designs for the Depropanizer, on one hand, and the ''imperfect y_2'' design for the F4d2 system, on the other hand), the modified ATDIMC designs reduce the overall IAE values and improve the robust performance indices of the original ATDIMC designs being modified. In situations where an ATDIMC design with a severe interaction effect on the least-desired output has an overall IAE value close to that of the dynamic decoupling IMC design (as is the case for the ''imperfect y_2'' design for the Depropanizer, on one hand, and the ''imperfect y_2'' design for the F4d2 system, on the other), the modified ATDIMC design can reduce the IAE value below that of the dynamic decoupling IMC design (as is the case with the ''imperfect y_1&y_2'' design for the Depropanizer that improves on the overall IAE value for the ''imperfect y_2'' design, on the one hand, and all the modified ATDIMC designs for the F4d2 System that improve on the overall IAE value for the ''imperfect y_2'' design'', on the other). As seen in the robustness values, however, while the modified ATDIMC designs lower the structured singular values for robust performance for the ATDIMC designs being modified, there is no guarantee that the resulting structured singular values will be better than those of dynamic decoupling IMC. In any case, as shown in Table 2, all designs satisfy the robustness requirements, even if some are more robust than others.

From the foregoing, it can be stated that for a stable $n \times n$ system with delays and RHP transmission zeros represented by an $n \times n$ transfer function matrix with rational-transfer-function-with-delay elements, the proposed triangular decoupling internal model control produces n different regular ATDIMC designs, on one hand, and $n-1$ modified ATDIMC designs per output whose ''imperfection'' is being modified, on the other. It is also clear that at least one of the regular ATDIMC designs outperforms the corresponding DIMC design for the same choice of tuning parameters as far as nominal and robustness characteristics are concerned. Indeed, the best ATDIMC design also outperforms the best of other dynamic-decoupling-based control techniques, as shown in the comparison of the technique with the MV-PID technique of [20].

It is also clear that in situations where the controlled systems have strong control-loop couplings, the strong couplings introduce pronounced disturbance-like effects on the least-desired output, making the overall IAE to grow significantly despite a successful shift of all inverse responses and interactions to that output. This is noticed in the design for ''imperfect y_3'' for the Depropanizer, on one hand, and the design for ''imperfect y_2'' for the F4d2 system, on the other. This is a shortcoming of the regular ATDIMC approach and the modified ATDIMC formulation was developed to reduce the severeness of the disturbance-like interaction effects. Admittedly, the modified ATDIMC does not guarantee that the overall IAE value will be lower than that of DIMC. A reformulation of the triangular decoupling problem using optimization techniques is likely to yield improved results for cases of severe interaction effects on the least-desired output. Also, a synthesis procedure that constrains the interaction effects on the least desired output is likely to yield better results for such situations.

The application of this technique to the model of the Depropanizer significantly shows that the formulation is applicable to a practical system. As shown, the best design using this technique is practically applicable to square multivariable systems with delays and RHP zeros. In all nonminimum-phase situations where DIMC is applicable, the ATDIMC is also applicable and has the potential of giving better results than DIMC.

VII. CONCLUSION

The proposed extended ATDIMC and modified ATDIMC concepts have been shown to achieve the set objectives of restricting the inverse response and interaction features to one and two outputs, respectively. It has also been shown that the overall error-index value of at least one ATDIMC design (the best design) is lower than that of the dynamic decoupling IMC technique for the same choice of tuning parameters least-desired output. These results are consistent with those in [37].

It can also be concluded that strong disturbance-like interaction effects can be noticed in the least-desired output in situations where control systems have strong control-loop couplings. The modified ATDIMC helps to reduce these effects but does not guarantee superiority to DIMC or dynamic-decoupling-based non-IMC designs. This is a shortcoming of the ATDIMC technique. However, based on the promise shown by the best ATDIMC design, optimization-based techniques and robust synthesis techniques can be used to perform a reformulation of the triangular decoupling problem so that the interaction effects on the least-desired output can be constrained to an acceptable level.

As pointed out in Section IV, it can also be concluded that each of the elements of the transfer function matrix of each designed controller must be reduced to a rational-transfer-function-plus-delay. This means that an $n \times n$ system requires n^2 reductions. This is like the situation with simplified decoupling that requires reduction of the elements of the decoupler matrix and the ''apparent process'', as in [20]. However, as shown with the simulation examples, the best ATDIMC design for a system with delays and RHP transmission zeros outperforms the best of simplified decoupling and other dynamic-decoupling-based techniques. As the dimensions increase, the advantages of using dynamic-decoupling-based and triangular-decoupling-based techniques will significantly reduce compared with the computational effort. In situations of high dimensions, a decentralized/multiloop approach will be preferable for simplicity, even if the overall IAE value will

be higher than a technique based on dynamic decoupling or triangular decoupling.

Ultimately, as noted in [3], the best MIMO IMC performance will always be achieved based on a technique of factorization such as inner-outer factorization. Extensions of IMC to linear and nonlinear nonminimum-phase systems with or without delays ultimately must consider equivalents of inner-outer factorization for optimum performance. However, as seen in the designs for delay-free nonminimum-phase systems, the design process for inner-outer-factorization-based IMC is computationally intensive and leads to more complex controllers than those obtained using dynamic-decoupling-based or triangular-decoupling-based techniques. In addition, the development of an analytical technique for performing inner-outer factorization for multivariable systems with delays is a difficult task, meaning that the only techniques in existence for extending the celebrated characteristics of IMC to square stable multivariable systems with delays and RHP transmission zeros are based on either dynamic decoupling (as seen in [11], [12], [14], and [15]) or triangular decoupling, as has been shown in both [37] and this study.

$$C_{11,1} = \frac{0.02421\,(4.2488s+1)\,(86.8672s+1)\,(95.875s+1)}{(s+0.0120061)\,(14.9671s+1)\,(64.657s+1)\,(\tau_1 s+1)} \tag{B1-2}$$

$$C_{12,1} = \frac{1.86421\,(86.8672s+1)\,(95.875s+1)}{(48.375s+1)\,(103.625s+1)\,(\tau_2 s+1)} \tag{B1-3}$$

$$C_{13,1} = \frac{1.05709\,(86.8672s+1)\,(95.875s+1)}{(63.3672s+1)\,(99.0021s+1)\,(\tau_3 s+1)} \tag{B1-4}$$

$$C_{21,1} = \frac{0.005762\,(20s+1)\,(86.8672s+1)\,(95.875s+1)\,e^{-57s}}{(s+0.0120061)\,(11.99s+1)\,(19.75s+1)\,(24.72s+1)\,(54.48s+1)\,(\tau_1 s+1)}, \tag{B1-5}$$

$$C_{22,1} = \frac{0.116745\,(-123.73s+1)\,(86.87s+1)\,(95.88s+1)\,e^{-24.5s}}{(49.25s+1)\,(49.5s+1)\,(79s+1)\,(\tau_2 s+1)} \tag{B1-6}$$

$$C_{23,1} = \frac{0.120804\,(-19.375s+1)\,(-14.25s+1)\,(86.8672s+1)\,(95.875s+1)\,e^{-5s}}{(30.1875s+1)\,(30.5s+1)\,(41.75s+1)\,(92.9375s+1)\,(\tau_3 s+1)} \tag{B1-7}$$

$$C_{31,1} = \frac{0.0924557\,(8s+1)\,(86.8672s+1)\,(95.875s+1)\,e^{-6s}}{(s+0.0120061)\,(23.37s+1)\,(24.29s+1)\,(40.18s+1)\,(44.61s+1)\,(\tau_1 s+1)} \tag{B1-8}$$

$$C_{32,1} = \frac{3.52011\,(-16.75s+1)\,(-5s+1)\,(86.8672s+1)\,(95.875s+1)\,e^{-10.53s}}{(30.125s+1)\,(30.5s+1)\,(45.125s+1)\,(93.875s+1)\,(\tau_2 s+1)} \tag{B1-9}$$

$$C_{33,1} = \frac{0.597495\,(-6s+1)\,(-5s+1)\,(86.87s+1)\,(95.88s+1)\,(180s+1)\,e^{-26s}}{(26s+1)\,(48s+1)\,(102s+1)\,(126s+1)\,(\tau_3 s+1)}. \tag{B1-10}$$

$$C_{11,2} = \frac{2.01714\,(-87.75s+1)\,(86.87\mathrm{s}+1)\,(95.88\mathrm{s}+1)\,e^{-16s}}{(120.9824s+1)\,(75.4844s+1)\,(\tau_1 s+1)} \tag{B2-2}$$

$$C_{12,2} = \frac{0.0223818(0.778s+1)(86.8672s+1)(95.875s+1)e^{-27s}}{(\mathrm{s}+0.0120061)(17.5129s+1)(112.1701s+1)(\tau_2 s+1)} \tag{B2-3}$$

$$C_{13,2} = \frac{1.05709\,(86.8672s+1)\,(95.875s+1)\,e^{-14.75s}}{(73.0313s+1)\,(113.453s+1)\,(\tau_3 s+1)} \tag{B2-4}$$

$$C_{21,2} = \frac{0.47989(86.8672s+1)(95.875s+1)e^{-14.9966s}}{(20.5002s+1)(91.5s+1)(\tau_1 s+1)} \tag{B2-5}$$

$$C_{22,2} = \frac{0.001401\,(-2.6612s+1)\,(86.8672s+1)(95.875s+1)}{(\mathrm{s}+0.0120061)(6.5784s+1)(78.2277s+1)(\tau_2 s+1)} \tag{B2-6}$$

$$C_{23,2} = \frac{0.120804(86.8672s+1)(95.875s+1)}{(82.1221s+1)(83.375s+1)\,(\tau_3 s+1)} \tag{B2-7}$$

$$C_{31,2} = \frac{7.70073(86.8672s+1)(95.875s+1)}{(62.9922s+1)(124s+1(\tau_1 s+1)} \tag{B2-8}$$

$$C_{32,2} = \frac{0.0422627(14.1653s+1)(86.8672s+1)(95.875s+1)e^{-2.5s}}{(\mathrm{s}+0.0120061)(60.6375s+1)(94.8681s+1)(\tau_2 s+1)} \tag{B2-9}$$

$$C_{33,2} = \frac{0.597495(-262.3s+1)(86.87s+1)(95.88s+1)e^{-91.5s}}{(128.5s+1)(0.1s+1)\,(\tau_3 s+1)}. \tag{B2-10}$$

APPENDIX A
PROOFS OF PROPOSITIONS 1 AND 2
APPENDIX A1: PROOF OF PROPOSITION 1

From Eq. (32),

$$C_{n\times n,n,init1}(s) = G^{-1}(s)H_{n\times n,n} \times \begin{bmatrix} H_{11}(s) & 0 & \dots & 0 & 0 \\ 0 & H_{22}(s) & \dots & 0 & 0 \\ \vdots & \vdots & \ddots & \vdots & \vdots \\ 0 & 0 & \dots & H_{n-1,n-1}(s) & 0 \\ H_{n1}(s) & H_{n2}(s) & \dots & H_{n,n-1}(s) & H_{nn}(s) \end{bmatrix} \tag{A1-1}$$

$$C_{n\times n,n,init1}(s) = \frac{P(s)}{(-s+z)M(s)} \cdot \begin{bmatrix} \hat{g}_{11}(s) & \hat{g}_{12}(s) & \dots & \hat{g}_{1n}(s) \\ \hat{g}_{21}(s) & \hat{g}_{22}(s) & \dots & \hat{g}_{2n}(s) \\ \vdots & \vdots & \ddots & \vdots \\ \hat{g}_{n1}(s) & \hat{g}_{n2}(s) & \dots & \hat{g}_{nn}(s) \end{bmatrix}$$

where

$$\left.\begin{aligned} H_{kk} &= \frac{e^{-\theta_k s}}{\tau_k s+1}; k = 1, \dots, n-1 \\ H_{np} &= \frac{s.a_{n,p}}{(s+z)} . \frac{e^{-\theta_p s}}{\tau_p s+1}; p = 1, \dots, n-1 \\ H_{nn} &= \frac{-s+z}{s+z} . \frac{e^{-\theta_n s}}{\tau_n s+1} \end{aligned}\right\} . \tag{A1-2}$$

$$C_{11,3} = \frac{2.01714(-249s+1)(86.8672s+1)(95.875s+1)e^{-0.3281s}}{(52.002s+1)(87s+1)(107.5s+1)(\tau_1 s+1)} \tag{B3-2}$$

$$C_{12,3} = \frac{1.86421(-54.5s+1)(86.8672s+1)(95.875s+1)e^{-13.8324s}}{(56.125s+1)(76s+1)(114.25s+1)(\tau_2 s+1)} \tag{B3-3}$$

$$C_{13,3} = \frac{0.0126915(4.9874s+1)(86.8672s+1)(95.875s+1)e^{-25.5s}}{(s+0.0120061)(54.0078s+1)(108.282s+1)(\tau_3 s+1)} \tag{B3-4}$$

$$C_{21,3} = \frac{0.479895(-30s+1)(86.8672s+1)(95.875s+1)e^{-4.64s}}{(82s+1)(91.25s+1)(95.25s+1)(\tau_1 s+1)} \tag{B3-5}$$

$$C_{22,3} = \frac{0.116744(-193.25s+1)(86.87s+1)(95.88s+1)e^{-18.07s}}{(83.498s+1)(84.25s+1)(84.5s+1)(\tau_2 s+1)} \tag{B3-6}$$

$$C_{23,3} = \frac{0.0014507(7.5s+1)(86.8672s+1)(95.875s+1)}{(s+0.0120061)(20.71s+1)(23.15s+1)(80.21s+1)(81.33s+1)(\tau_3 s+1)} \tag{B3-7}$$

$$C_{31,3} = \frac{7.70073(-25.4688s+1)(86.8672s+1)(95.875s+1)(225.25s+1)}{(33.25s+1)(43.25s+1)(95.5s+1)(134.375s+1)(\tau_1 s+1)} \tag{B3-8}$$

$$C_{32,3} = \frac{3.52142(-25.73s+1)(86.8672s+1)(95.875s+1)(211.5s+1)}{(38.0625s+1)(1+43s)(1+102s)(1+124.998s)(\tau_2 s+1)} \tag{B3-9}$$

$$C_{33,3} = \frac{0.00717992(86.8672s+1)(95.875s+1)(386s+1)e^{-5.5s}}{(s+0.0120061)(42.69s+1)(46.805s+1)(136.63s+1)(\tau_3 s+1)}. \tag{B3-10}$$

$$C_{11,12} = \frac{0.024218(4.2488s+1)(86.8672s+1)(95.875s+1)}{(s+0.0120061)(14.9671s+1)(64.657s+1)(\tau_1 s+1)} \tag{B4-2}$$

$$C_{12,12} = \frac{0.0223818(0.778s+1)(86.8672s+1)(95.875s+1)e^{-27s}}{(s+0.0120061)(17.5129s+1)(112.1701s+1)(\tau_2 s+1)} \tag{B4-3}$$

$$C_{13,12} = \frac{1.05709(86.8672s+1)(95.875s+1)e^{-14.75s}}{(73.0313s+1)(113.453s+1)(\tau_3 s+1)} \tag{B4-4}$$

$$C_{21,2} = \frac{0.00576166(20s+1)(86.8672s+1)(95.875s+1)e^{-57s}}{(s+0.0120061)(11.9847s+1)(19.747s+1)(24.7244s+1)(54.4759s+1)(\tau_1 s+1)} \tag{B4-5}$$

$$C_{22,12} = \frac{0.001401(-2.6612s+1)(86.8672s+1)(95.875s+1)}{(s+0.0120061)(6.5784s+1)(78.2277s+1)(\tau_2 s+1)} \tag{B4-6}$$

$$C_{23,12} = \frac{0.120804(86.8672s+1)(95.875s+1)}{(82.1221s+1)(83.375s+1)(\tau_3 s+1)} \tag{B4-7}$$

$$C_{31,12} = \frac{0.0924557(8s+1)(86.8672s+1)(95.875s+1)e^{-6s}}{(s+0.0120061)(23.3672s+1)(24.2855s+1)(40.1834s+1)(44.6128s+1)(\tau_1 s+1)} \tag{B4-8}$$

$$C_{32,12} = \frac{0.0422627(14.1653s+1)(86.8672s+1)(95.875s+1)e^{-2.5s}}{(s+0.0120061)(60.6375s+1)(94.8681s+1)(\tau_2 s+1)} \tag{B4-9}$$

$$C_{33,12} = \frac{0.597495(-262.3s+1)(86.87s+1)(95.88s+1)e^{-91.5s}}{(128.5s+1)(0.1s+1)(\tau_3 s+1)}. \tag{B4-10}$$

Combining the 2 matrices in Eq. (A1-1) yields

$$C_{n\times n,n,init1}(s) = \frac{P(s)}{(-s+z)M(s)} \times \begin{bmatrix} K_{11} & K_{12} & \dots & K_{1,n-1} & K_{1n} \\ K_{21} & K_{22} & \dots & K_{2,n-1} & K_{2n} \\ \vdots & \vdots & \ddots & \vdots & \vdots \\ K_{n-1,1} & K_{n-1,2} & \dots & K_{n-1,n-1} & K_{n-1,n} \\ K_{n1} & K_{n2} & \dots & K_{n,n-1} & K_{nn} \end{bmatrix} \quad \text{(A1-3)}$$

where

$$K_{\gamma q}(s) = v_{\gamma q}(s)\frac{e^{-\theta_q s}}{\tau_q s+1} = \left(\hat{g}_{\gamma q}(s) + \hat{g}_{\gamma n}(s).\frac{s.a_{n,q}(s)}{(s+z)}\right)\frac{e^{-\theta_q s}}{\tau_q s+1}; \quad \gamma = 1,2,\dots,n;\ q = 1,2,\dots,n-1 \quad \text{(A1-4)}$$

$$K_{\gamma n}(s) = \hat{g}_{\gamma n}.\frac{-s+z}{s+z}.\frac{e^{-\theta_n s}}{\tau_n s+1}, \gamma = 1,2,\dots,n. \quad \text{(A1-5)}$$

$$C_{11,13} = \frac{0.024218(4.2488s+1)(86.8672s+1)(95.875s+1)}{(s+0.0120061)(14.9671s+1)(64.657s+1)(\tau_1 s+1)} \quad \text{(B5-2)}$$

$$C_{12,13} = \frac{1.86421(-54.5s+1)(86.8672s+1)(95.875s+1)e^{-13.8324s}}{(56.125s+1)(76s+1)(114.25s+1)(\tau_2 s+1)} \quad \text{(B5-3)}$$

$$C_{13,13} = \frac{0.0126915(4.9874s+1)(86.8672s+1)(95.875s+1)e^{-25.5s}}{(s+0.0120061)(54.0078s+1)(108.282s+1)(\tau_3 s+1)} \quad \text{(B5-4)}$$

$$C_{21,13} = \frac{0.00576166(20s+1)(86.8672s+1)(95.875s+1)e^{-57s}}{(s+0.0120061)(11.98s+1)(19.75s+1)(24.72s+1)(54.48s+1)(\tau_1 s+1)} \quad \text{(B5-5)}$$

$$C_{22,13} = \frac{0.116744(-193.25s+1)(86.8672s+1)(95.875s+1)e^{-18.0716s}}{(83.498s+1)(84.25s+1)(84.5s+1)(\tau_2 s+1)} \quad \text{(B5-6)}$$

$$C_{23,13} = \frac{0.0014507(7.5s+1)(86.8672s+1)(95.875s+1)}{(s+0.0120061)(20.71s+1)(23.15s+1)(80.22s+1)(81.33s+1)(\tau_3 s+1)} \quad \text{(B5-7)}$$

$$C_{31,13} = \frac{0.0924557(8s+1)(86.8672s+1)(95.875s+1)e^{-6s}}{(s+0.0120061)(23.37s+1)(24.29s+1)(40.18s+1)(44.61s+1)(\tau_1 s+1)} \quad \text{(B5-8)}$$

$$C_{32,13} = \frac{3.52142(-25.7344s+1)(86.8672s+1)(95.875s+1)(211.5s+1)}{(38.0625s+1)(43s+1)(102s+1)(124.998s+1)(\tau_2 s+1)} \quad \text{(B5-9)}$$

$$C_{33,13} = \frac{0.00717992(86.8672s+1)(95.875s+1)(386s+1)e^{-5.5s}}{(s+0.0120061)(42.6858s+1)(46.8048s+1)(136.629s+1)(\tau_3 s+1)}. \quad \text{(B5-10)}$$

$$C_{11,23} = \frac{2.01714(-249s+1)(86.8672s+1)(95.875s+1)e^{-0.3281s}}{(52.002s+1)(87s+1)(107.5s+1)(\tau_1 s+1)} \quad \text{(B6-2)}$$

$$C_{12,23} = \frac{0.0223818(0.778s+1)(86.8672s+1)(95.875s+1)e^{-27s}}{(s+0.0120061)(17.5129s+1)(112.17s+1)(\tau_2 s+1)} \quad \text{(B6-3)}$$

$$C_{13,23} = \frac{0.0126915(4.9874s+1)(86.8672s+1)(95.875s+1)e^{-25.5s}}{(s+0.0120061)(54.0078s+1)(108.282s+1)(\tau_3 s+1)} \quad \text{(B6-4)}$$

$$C_{21,23} = \frac{0.479895(-30s+1)(86.8672s+1)(95.875s+1)e^{-4.64s}}{(82s+1)(91.25s+1)(95.25s+1)(\tau_1 s+1)} \quad \text{(B6-5)}$$

$$C_{22,23} = \frac{0.001401(-2.6612s+1)(86.8672s+1)(95.875s+1)}{(s+0.0120061)(6.5784s+1)(78.2277s+1)(\tau_2 s+1)} \quad \text{(B6-6)}$$

$$C_{23,23} = \frac{0.0014507(7.5s+1)(86.8672s+1)(95.875s+1)}{(s+0.0120061)(20.71s+1)(23.15s+1)(80.22s+1)(81.33s+1)(\tau_3 s+1)} \quad \text{(B6-7)}$$

$$C_{31,23} = \frac{7.70073(-25.4688s+1)(86.8672s+1)(95.875s+1)(225.25s+1)}{(33.25s+1)(43.25s+1)(95.5s+1)(134.375s+1)(\tau_1 s+1)} \quad \text{(B6-8)}$$

$$C_{32,23} = \frac{0.0422628(14.1653s+1)(86.8672s+1)(95.875s+1)e^{-2.5s}}{(s+0.0120061)(60.6375s+1)(94.8681s+1)(\tau_2 s+1)} \quad \text{(B6-9)}$$

$$C_{33,23} = \frac{0.00717992(86.8672s+1)(95.875s+1)(386s+1)e^{-5.5s}}{(s+0.0120061)(42.69s+1)(46.805s+1)(136.63s+1)(\tau_3 s+1)}. \quad \text{(B6-10)}$$

Rewriting Eqs. (A1-3) to (A1-5) in block matrix form yields

$$C_{n\times n,n,init1}(s) = \frac{P(s)}{(-s+z)M(s)} \times \begin{bmatrix} \boldsymbol{v_1}F_1 & \boldsymbol{v_2}F_2 & \dots & \boldsymbol{v_{n-1}}F_{n-1} & \hat{\mathbf{g}}_{\boldsymbol{n}}\mathrm{Fm}_n \end{bmatrix} \quad \text{(A1-6)}$$

where

$$\boldsymbol{v_q} = \begin{bmatrix} v_{1q} & v_{2q} & \dots & v_{nq} \end{bmatrix}^T \quad \text{(A1-7)}$$

$$\hat{\mathbf{g}}_{\boldsymbol{n}} = \begin{bmatrix} \hat{\mathrm{g}}_{1n} & \hat{\mathrm{g}}_{2n} & \dots & \hat{\mathrm{g}}_{nn} \end{bmatrix}^T \quad \text{(A1-8)}$$

$$F_q = \frac{e^{-\theta_q s}}{\tau_q s+1}; \quad q = 1,\dots,n-1 \quad \text{(A1-9)}$$

$$\mathrm{Fm}_n = \frac{-s+z}{s+z}.\frac{e^{-\theta_n s}}{\tau_n s+1}. \quad \text{(A1-10)}$$

APPENDIX A2: PROOF OF PROPOSITION 2

$$C_{n\times n,i,init1}(s) = G^{-1}(s)H_{n\times n,i}$$

$$C_{n\times n,i,init1}(s) = \frac{P(s)}{(-s+z)M(s)} \cdot \begin{bmatrix} \hat{\mathrm{g}}_{11}(s) & \hat{\mathrm{g}}_{12}(s) & \dots & \hat{\mathrm{g}}_{1n}(s) \\ \hat{\mathrm{g}}_{21}(s) & \hat{\mathrm{g}}_{22}(s) & \dots & \hat{\mathrm{g}}_{2n}(s) \\ \vdots & \vdots & \ddots & \vdots \\ \hat{\mathrm{g}}_{n1}(s) & \hat{\mathrm{g}}_{n2}(s) & \dots & \hat{\mathrm{g}}_{nn}(s) \end{bmatrix} \alpha(s), \quad \text{(A2-1)}$$

where

$\alpha(s)$

$$= \begin{bmatrix} H_{11} & 0 & \dots & 0 & 0 & 0 & \dots & 0 & 0 \\ 0 & H_{22} & \dots & 0 & 0 & 0 & \dots & 0 & 0 \\ \vdots & \vdots & \ddots & \vdots & \vdots & \vdots & \dots & 0 & 0 \\ 0 & 0 & \dots & H_{i-1,i-1} & 0 & 0 & \dots & 0 & 0 \\ H_{i1} & H_{i2} & \dots & H_{i,i-1} & H_{ii} & H_{i,i+1} & \dots & H_{i,n-1} & H_{in} \\ 0 & 0 & \dots & 0 & 0 & H_{i+1,i+1} & \dots & 0 & 0 \\ \vdots & \vdots & \vdots & \vdots & \vdots & \vdots & \ddots & \vdots & \vdots \\ 0 & 0 & \dots & 0 & 0 & 0 & 0 & H_{n-1,n-1} & 0 \\ 0 & 0 & \dots & 0 & 0 & 0 & 0 & 0 & H_{nn} \end{bmatrix} \quad \text{(A2-2)}$$

where

$$\left.\begin{aligned} H_{kk} &= \frac{e^{-\theta_k s}}{\tau_k s+1}; k = 1,\dots,i-1,i+1,\dots,n \\ H_{ir} &= \frac{s.a_{i,r}}{(s+z)}.\frac{e^{-\theta_r s}}{\tau_r s+1}; r = 1,\dots,i-1,i+1,\dots,n \\ H_{ii} &= \frac{-s+z}{s+z}.\frac{e^{-\theta_i s}}{\tau_i s+1} \end{aligned}\right\}. \quad \text{(A2-3)}$$

Combining the 2 matrices in Eq. (A2-1) yields

$$C_{n\times n,i,init1}(s) = \frac{P(s)}{(-s+z)M(s)} \begin{bmatrix} W_{11} & \cdots & W_{1n} \\ \vdots & \ddots & \vdots \\ W_{n1} & \cdots & W_{nn} \end{bmatrix} \quad \text{(A2-4)}$$

where

$$W_{wr}(s) = v_{wr}(s)\frac{e^{-\theta_q s}}{\tau_q s+1} = \left(\hat{\mathrm{g}}_{wr}(s) + \hat{\mathrm{g}}_{wi}(s).\frac{s.a_{i,q}(s)}{(s+z)}\right)\frac{e^{-\theta_q s}}{\tau_q s+1}$$

$$C_{11,dd} = \frac{0.024218(4.2488s+1)(86.8672s+1)(95.875s+1)}{(s+0.0120061)(14.9671s+1)(64.657s+1)(\tau_1 s+1)} \quad \text{(B7-2)}$$

$$C_{12,dd} = \frac{0.02238185(0.778s+1)(86.8672s+1)(95.875s+1)e^{-27s}}{(s+0.0120061)(112.1701s+1)(17.5129s+1)(\tau_2 s+1)} \quad \text{(B7-3)}$$

$$C_{13,dd} = \frac{0.0126915(4.9874s+1)(86.8672s+1)(95.875s+1)e^{-25.5s}}{(s+0.0120061)(54.0078s+1)(108.282s+1)(\tau_3 s+1)} \quad \text{(B7-4)}$$

$$C_{21,dd} = \frac{0.00576166(20s+1)(86.8672s+1)(95.875s+1)e^{-57s}}{(s+0.0120061)(11.985s+1)(19.75s+1)(24.724s+1)(54.48s+1)(\tau_1 s+1)} \quad \text{(B7-5)}$$

$$C_{22,dd} = \frac{0.001401(-2.6612s+1)(86.8672s+1)(95.875s+1)}{(s+0.0120061)(6.5784s+1)(78.2277s+1)(\tau_2 s+1)} \quad \text{(B7-6)}$$

$$C_{23,dd} = \frac{0.0014507(7.5s+1)(86.8672s+1)(95.875s+1)}{(s+0.0120061)(20.71s+1)(23.15s+1)(80.22s+1)(81.33s+1)(\tau_3 s+1)} \quad \text{(B7-7)}$$

$$C_{31,dd} = \frac{0.0924557(8s+1)(86.8672s+1)(95.875s+1)e^{-6s}}{(s+0.0120061)(23.37s+1)(24.29s+1)(40.18s+1)(44.61s+1)(\tau_1 s+1)} \quad \text{(B7-8)}$$

$$C_{32,dd} = \frac{0.04226275(14.1653s+1)(86.8672s+1)(95.875s+1)e^{-2.5s}}{(s+0.0120061)(94.8681s+1)(60.6375s+1)(\tau_2 s+1)} \quad \text{(B7-9)}$$

$$C_{33,dd} = \frac{0.00717992(86.8672s+1)(95.875s+1)(386s+1)e^{-5.5s}}{(s+0.0120061)(42.6858s+1)(46.8048s+1)(136.629s+1)(\tau_3 s+1)}. \quad \text{(B7-10)}$$

$$w = 1, 2, \ldots, n; \quad r = 1, \ldots, i-1,\ i+1, \ldots, n \tag{A2-5}$$

$$W_{wi}(s) = \hat{\mathrm{g}}_{wi}(s).\frac{-s+z}{s+z}.\frac{e^{-\theta_i s}}{\tau_i s+1}, \quad r = i. \tag{A2-6}$$

Rewriting Eqs. (A1-4) to (A1-6) in block matrix form yields

$$\begin{aligned} &C_{n\times n,i,init1}\,(s) \\ &= \frac{P\,(s)}{(-s+z)\,M\,(s)} \\ &\times \left[\boldsymbol{v_1}F_1 \quad \ldots \quad \boldsymbol{v_{i-1}}F_{i-1} \quad \boldsymbol{v_{i+1}}F_{i+1} \quad \cdots \quad \boldsymbol{v_n}F_n \quad \hat{\mathrm{g}}_{\boldsymbol{i}}\mathrm{Fm}_i\right] \end{aligned} \tag{A2-7}$$

where

$$\boldsymbol{v_r} = \begin{bmatrix} v_{1r} & v_{2r} & \ldots & v_{nr} \end{bmatrix}^T \tag{A2-8}$$

$$F_r = \frac{e^{-\theta_r s}}{\tau_r s+1}; \quad r = 1, \ldots, i-1,\ i+1, \ldots, n \tag{A2-9}$$

$$\hat{\mathrm{g}}_{\boldsymbol{i}} = \begin{bmatrix} \hat{\mathrm{g}}_{1i} & \hat{\mathrm{g}}_{2i} & \ldots & \hat{\mathrm{g}}_{ni} \end{bmatrix}^T \tag{A2-10}$$

$$\mathrm{Fm}_i = \frac{-s+z}{s+z}.\frac{e^{-\theta_i s}}{\tau_i s+1}. \tag{A2-11}$$

$$C_{11,1} = \frac{0.00611518(s+1)^2(16.9688s+1)(17.375s+1)e^{-5.25s}}{(0.1133s+1)(0.25s+1)(s+0.0432123)(5.25s+1)(10.25s+1)\,(\tau_1 s+1)} \tag{C1-2}$$

$$C_{12,1} = \frac{0.0154741(0.2817s+1)(0.375s+1)(16.9688s+1)(17.375s+1)}{(0.1133s+1)(0.25s+1)(10s+1)(100s+1)\,(\tau_2 s+1)} \tag{C1-3}$$

$$C_{13,1} = \frac{0.0310904(-0.7969s+1)(-0.6406s+1)(16.9688s+1)(69s+1)e^{-8.875s}}{(0.1133s+1)(0.25s+1)(11.625s+1)(16.998s+1)\,(\tau_3 s+1)} \tag{C1-4}$$

$$C_{14,1} = \frac{-0.0997113(0.7656s+1)(0.9922s+1)(16.9688s+1)(17.375s+1)}{(0.1133s+1)(0.25s+1)(22.9766s+1)(23.9922s+1)\,(\tau_4 s+1)} \tag{C1-5}$$

$$C_{21,1} = \frac{0.004593(-4.8125s+1)(4.7548s+1)(16.9688s+1)(17.375s+1)e^{-12.5s}}{(0.1133s+1)(0.25s+1)(s+0.0432123)(6s+1)(6.2539s+1)\,(\tau_1 s+1)} \tag{C1-6}$$

$$C_{22,1} = \frac{-0.0616478(0.2625s+1)(16.9688s+1)(17.375s+1)e^{-14.89s}}{(0.1133s+1)(0.25s+1)(313.938s^2+24.498s+1)\,(\tau_2 s+1)} \tag{C1-7}$$

$$C_{23,1} = \frac{0.021459(3.3255s+1)(16.9688s+1)(17.375s+1)(104s+1)e^{-28.88s}}{(0.1133s+1)(0.25s+1)(14s+1)(18.9375s+1)\,(\tau_3 s+1)} \tag{C1-8}$$

$$C_{24,1} = \frac{-0.0152609(-86.69s+1)(1.57s+1)(16.969s+1)(17.375s+1)e^{-28.25s}}{(0.1133s+1)(0.25s+1)(17.4844s+1)(18.625s+1)\,(\tau_4 s+1)} \tag{C1-9}$$

$$C_{31,1} = \frac{0.00765788(s+1)(16.9688s+1)(17.375s+1)e^{-12.501s}}{(0.1133s+1)(0.25s+1)(s+0.0432123)(136.8s^2+18.84s+1)\,(\tau_1 s+1)} \tag{C1-10}$$

$$C_{32,1} = \frac{0.0533(-0.725s+1)(-0.592s+1)(-0.525s+1)(16.97s+1)(17.38s+1)e^{-25.36s}}{(0.1133s+1)(0.25s+1)(16.0993s+1)(16.3358s+1)(16.8149s+1)\,(\tau_2 s+1)} \tag{C1-11}$$

$$C_{33,1} = \frac{-0.0715523(-13.19s+1)(-0.656s+1)(-0.602s+1)(16.97s+1)(17.375s+1)e^{-33.38s}}{(0.1133s+1)(0.25s+1)(12s+1)(12.75s+1)(12.875s+1)\,(\tau_3 s+1)} \tag{C1-12}$$

$$C_{34,1} = \frac{0.0402176(-1.125s+1)(-0.5s+1)(16.9688s+1)(17.375s+1)(62.2499s+1)e^{-25.38s}}{(0.1133s+1)(0.25s+1)(15.25s+1)(16.625s+1)(18.5s+1)\,(\tau_4 s+1)} \tag{C1-13}$$

$$C_{41,1} = \frac{-0.0110499(0.2501s+1)(16.9688s+1)(17.375s+1)}{(0.1133s+1)(s+0.0432123)(7.5s+1)(9.3124s+1)\,(\tau_1 s+1)} \tag{C1-14}$$

$$C_{42,1} = \frac{\begin{bmatrix} -0.0121119(-5.7046s+1)(-2.25s+1)(-2.0714s+1)(-1.4392s+1) \\ (-1.4151s+1)(16.9688s+1)(17.375s+1) \end{bmatrix}}{\begin{bmatrix} (0.1133s+1)(0.25s+1)(4.5767s+1)(5.0133s+1) \\ (6.9103s+1)(7.9433s+1)(23.4457s+1) \end{bmatrix}(\tau_2 s+1)} \tag{C1-15}$$

$$C_{43,1} = \frac{\begin{bmatrix} (0.104841(-5.8125s+1)(-3.8125s+1)(-3.4375s+1)(-1.9688s+1) \\ (-1.8672s+1)(16.9688s+1)(17.375s+1) \end{bmatrix}}{\begin{bmatrix} (0.1133s+1)(0.25s+1)(6.5313s+1) \\ (7s+1)^2(8.4453s+1)(18.5s+1) \end{bmatrix}(\tau_3 s+1)} \tag{C1-16}$$

$$C_{44,1} = \frac{(0.0816345(-11.125s+1)(-1.9824s+1)(-0.75s+1)(16.9688s+1)(17.375s+1)e^{-10s}}{(0.1133s+1)(0.25s+1)(10.0625s+1)(18s+1)(18.75s+1)\,(\tau_4 s+1)}. \tag{C1-17}$$

APPENDIX B
CONTROLLER MATRIX DETAILS FOR DESIGNS FOR THE 3 × 3 DEPROPANIZER

APPENDIX B1: CONTROLLER MATRIX FOR ATDIMC DESIGN ACHIEVING "IMPERFECT y_1" FOR 3 × 3 DEPROPANIZER

Using the procedure in Section III-B ($i = 1$), the ATDIMC controller achieving "imperfect y_1" for 3 × 3 Depropanizer was computed as

$$C_{3\times3.1}(s) = \begin{bmatrix} C_{11,1}(s) & C_{12,1}(s) & C_{13,1}(s) \\ C_{21,1}(s) & C_{22,1}(s) & C_{23,1}(s) \\ C_{31,1}(s) & C_{32,1}(s) & C_{33,1}(s) \end{bmatrix} \quad \text{(B1-1)}$$

where as B1-2–B1-10, shown at the bottom of page 15.

APPENDIX B2: CONTROLLER MATRIX FOR ATDIMC DESIGN ACHIEVING "IMPERFECT y_2" FOR 3 × 3 DEPROPANIZER

Using the procedure in Section III-B ($i = 2$), the ATDIMC controller achieving "imperfect y_2" was computed as

$$C_{3\times3.2}(s) = \begin{bmatrix} C_{11,2}(s) & C_{12,2}(s) & C_{13,2}(s) \\ C_{21,2}(s) & C_{22,2}(s) & C_{23,2}(s) \\ C_{31,2}(s) & C_{32,2}(s) & C_{33,2}(s) \end{bmatrix} \quad \text{(B2-1)}$$

where as B2-2–B2-10, shown at the bottom of page 15.

$$C_{11,2} = \frac{0.141506(-13.25s+1)(2.6565s+1)(16.9688s+1)(17.375s+1)(63s+1)e^{-2.2168s}}{(0.1133s+1)(0.25s+1)(19s+1)(19.875s+1)(20.3125s+1)(\tau_1 s+1)} \quad \text{(C2-2)}$$

$$C_{12,2} = \frac{0.000668673(-0.5002s+1)(16.9688s+1)(17.375s+1)98s+1)e^{-2.9415s}}{(0.1133s+1)(0.25s+1)(s+0.432123)(14.1249s+1)(14.7812s+1)(\tau_2 s+1)} \quad \text{(C2-3)}$$

$$C_{13,2} = \frac{0.0310904(1.9531s+1)(16.9688s+1)(17.375s+1)(54.0088s+1)}{(0.1133s+1)(0.25s+1)(11.7188s+1)(14.375s+1)(\tau_3 s+1)} \quad \text{(C2-4)}$$

$$C_{14,2} = \frac{-0.0997113(-6.8125s+1)(-3.2969s+1)(-2.3906s+1)(17.375s+1)(43.496s+1)}{(0.1133s+1)(0.25s+1)(11.9844s+1)(12.9688s+1)(18s+1)(\tau_4 s+1)} \quad \text{(C2-5)}$$

$$C_{21,2} = \frac{0.106285(5.945s+1)(16.9688s+1)(17.375s+1)(137.47s+1)e^{-32.9666s}}{(0.1133s+1)(0.25s+1)(16.7344s+1)(19.5s+1)(\tau_1 s+1)} \quad \text{(C2-6)}$$

$$C_{22,2} = \frac{-0.00266395(-9.6875s+1)(0.5s+1)(16.9688s+1)(17.375s+1)e^{-21.875s}}{(0.1133s+1)(0.25s+1)(s+0.0432123)(8.5s+1)(8.75s+1)(\tau_2 s+1)} \quad \text{(C2-7)}$$

$$C_{23,2} = \frac{0.021459(-183.608s+1)(-0.1011s+1)(4s+1)(16.969s+1)(17.375s+1)e^{-33.8682s}}{(0.1133s+1)(0.25s+1)(10s+1)(17.0938s+1)(17.3438s+1)(\tau_3 s+1)} \quad \text{(C2-8)}$$

$$C_{24,2} = \frac{-0.0152609(0.7495s+1)(16.9688s+1)(17.375s+1)(45.125s+1)(315s+1)e^{-29.82s}}{(0.1133s+1)(0.25s+1)(28s+1)^2(32s+1)(\tau_4 s+1)} \quad \text{(C2-9)}$$

$$C_{31,2} = \frac{0.177215(-17.9999s+1)(0.5s+1)(16.9688s+1)(17.375s+1)e^{-5.4668s}}{(0.1133s+1)(0.25s+1)(26s+1)(30.25s+1)(\tau_1 s+1)} \quad \text{(C2-10)}$$

$$C_{32,2} = \frac{0.00230408(-5.75s+1)(7.25s+1)(16.9688s+1)(17.375s+1)}{(0.1133s+1)(0.25s+1)(s+0.0432123)(19.5s+1)(22.75s+1)(\tau_2 s+1)} \quad \text{(C2-11)}$$

$$C_{33,2} = \frac{-0.0715523(-33.5039s+1)(3.002s+1)(16.9688s+1)(17.375s+1)e^{-12.375s}}{(0.1133s+1)(0.25s+1)(25.7499s+1)(27s+1)(\tau_3 s+1)} \quad \text{(C2-12)}$$

$$C_{34,2} = \frac{0.0402176(16.9688s+1)(17.375s+1)(103.398s+1)e^{-18.1868s}}{(0.1133s+1)(0.25s+1)(30.5002s+1)(32.4985s+1)(\tau_4 s+1)} \quad \text{(C2-13)}$$

$$C_{41,2} = \frac{-0.255712(-0.9941s+1)(-0.953s+1)(-0.875s+1)(16.97s+1)(17.375s+1)(45.89s+1)}{(0.1133s+1)(0.25s+1)(11.5625s+1)(12.125s+1)(12.633s+1)(14.094s+1)(\tau_1 s+1)} \quad \text{(C2-14)}$$

$$C_{42,2} = \frac{-0.000523385(s+1)(16.9688s+1)(17.375s+1)(129.875s+1)e^{-4.126s}}{(0.1133s+1)(0.25s+1)(s+0.0432123)(11.875s+1)(12.1875s+1)(\tau_2 s+1)} \quad \text{(C2-15)}$$

$$C_{43,2} = \frac{\begin{bmatrix} 0.104841(-1.6875s+1)(-1.6016s+1)(-1.3789s+1)(16.9688s+1) \\ (17.375s+1)(44.75s+1) \end{bmatrix} e^{-2.0156s}}{(0.1133s+1)(0.25s+1)(12.0898s+1)(12.4373s+1)(13.0938s+1)(14s+1)(\tau_3 s+1)} \quad \text{(C2-16)}$$

$$C_{44,4} = \frac{\begin{bmatrix} 0.0816345(-1.4531s+1)(-1.2263s+1)(-0.8513s+1)(16.9688s+1) \\ (17.375s+1)(48.0156s+1) \end{bmatrix} e^{-13.875s}}{(0.1133s+1)(0.25s+1)(11.48s+1)(12.0625s+1)(13.0938s+1)(13.375s+1)(\tau_4 s+1)}. \quad \text{(C2-17)}$$

APPENDIX B3: CONTROLLER MATRIX FOR ATDIMC DESIGN ACHIEVING "IMPERFECT y_3" FOR 3 × 3 DEPROPANIZER

Using the procedure in Section III-A, the ATDIMC controller achieving "imperfect y_3" for 3 × 3 Depropanizer was computed as

$$C_{3\times3.3}(s) = \begin{bmatrix} C_{11,3}(s) & C_{12,3}(s) & C_{13,3}(s) \\ C_{21,3}(s) & C_{22,3}(s) & C_{23,3}(s) \\ C_{31,3}(s) & C_{32,3}(s) & C_{33,3}(s) \end{bmatrix} \quad \text{(B3-1)}$$

where as B3-2–B3-10, shown at the bottom of page 16.

APPENDIX B4: CONTROLLER MATRIX FOR ATDIMC DESIGN ACHIEVING "IMPERFECT y_1&y_2" FOR 3 × 3 DEPROPANIZER

Using the procedure in Section III-D ($j = 1, i = 2$), the ATDIMC controller achieving "imperfect y_1&y_2" for 3 × 3 Depropanizer was computed as

$$C_{3\times3.12}(s) = \begin{bmatrix} C_{11,12}(s) & C_{12,12}(s) & C_{13,12}(s) \\ C_{21,12}(s) & C_{22,12}(s) & C_{23,12}(s) \\ C_{31,12}(s) & C_{32,12}(s) & C_{33,12}(s) \end{bmatrix} \quad \text{(B4-1)}$$

where as B4-2–B4-10, shown at the bottom of page 16.

APPENDIX B5: CONTROLLER MATRIX FOR ATDIMC DESIGN ACHIEVING "IMPERFECT y_1&y_3" FOR 3 × 3 DEPROPANIZER

Using the procedure in Section III-C ($j = 1, n = 3$), modified ATDIMC controllers achieving "imperfect y_1 & y_3" for 3×3 Depropanizer was computed as

$$C_{3\times3.13}(s) = \begin{bmatrix} C_{11,13}(s) & C_{12,13}(s) & C_{13,13}(s) \\ C_{21,13}(s) & C_{22,13}(s) & C_{23,13}(s) \\ C_{31,13}(s) & C_{32,13}(s) & C_{33,13}(s) \end{bmatrix} \quad \text{(B5-1)}$$

$$C_{11,3} = \frac{0.141506(-0.75s+1)(0.5s+1)(16.9688s+1)(17.375s+1)(67s+1)e^{-7.4374s}}{(0.1133s+1)(0.25s+1)(16s+1)(16.0005s+1)(16.5s+1)(\tau_1 s+1)} \quad \text{(C3-2)}$$

$$C_{12,3} = \frac{0.0154719(3.75s+1)(16.9688s+1)(17.375s+1)(153s+1)}{(0.1133s+1)(0.25s+1)(18.9688s+1)(21.875s+1)(\tau_2 s+1)} \quad \text{(C3-4)}$$

$$C_{13,3} = \frac{0.00134349(-20s+1)(16.9688s+1)(17.375s+1)(29.0078s+1)e^{-37.4932s}}{(0.1133s+1)(0.25s+1)(s+0.0432123)(19.9961s+1)(23.7324s+1)(\tau_3 s+1)} \quad \text{(C3-2)}$$

$$C_{14,3} = \frac{-0.0997113(7.1875s+1)(16.9688s+1)(17.375s+1)(50s+1)e^{-30s}}{(0.1133s+1)(0.25s+1)(18.25s+1)(24s+1)(\tau_4 s+1)} \quad \text{(C3-5)}$$

$$C_{21,3} = \frac{0.106285(4.5541s+1)(16.9688s+1)(17.375s+1)(70.2298s+1)e^{-31.7871s}}{(0.1133s+1)(0.25s+1)(7.9828s+1)(45.2332s+1)(\tau_1 s+1)} \quad \text{(C3-6)}$$

$$C_{22,3} = \frac{-0.0616478(-1.17s+1)(-1.09s+1)(-0.96s+1)(-0.5s+1)(16.97s+1)(17.375s+1)e^{-7.623s}}{(0.1133s+1)(0.25s+1)(7.125s+1)(7.75s+1)(8s+1)^2(\tau_2 s+1)} \quad \text{(C3-7)}$$

$$C_{23,3} = \frac{0.0009273(-7.5418s+1)(16.9688s+1)(17.375s+1)(60.1769s+1)e^{-43.6871s}}{(0.1133s+1)(0.25s+1)(s+0.0432123)(7.0857s+1)(59.912s+1)(\tau_3 s+1)} \quad \text{(C3-8)}$$

$$C_{24,3} = \frac{-0.0152609(-2.3125s+1)^2(-1.6719s+1)(16.9688s+1)(17.375s+1)(82s+1)e^{-13s}}{(0.1133s+1)(0.25s+1)(8s+1)(9s+1)(10s+1)(12s+1)(\tau_4 s+1)} \quad \text{(C3-9)}$$

$$C_{31,3} = \frac{0.177215(-1.8789s+1)(-0.5s+1)(16.9688s+1)(17.375s+1)e^{-7.1249s}}{(0.1133s+1)(0.25s+1)(28.5938s+1)(30s+1)(\tau_1 s+1)} \quad \text{(C3-10)}$$

$$C_{32,3} = \frac{0.05332(8.2129s+1)(16.9688s+1)(17.375s+1)e^{-14.034s}}{(0.1133s+1)(0.25s+1)(42.2791s+1)(\tau_2 s+1)} \quad \text{(C3-11)}$$

$$C_{33,3} = \frac{-0.00309194(0.5s+1)(s+1)(16.9688s+1)(17.375s+1)e^{-21.75s}}{(0.1133s+1)(0.25s+1)(s+0.0432123)(21s+1)(21.9927s+1)(\tau_3 s+1)} \quad \text{(C3-12)}$$

$$C_{34,3} = \frac{0.0402176(-5.2383s+1)(-0.8916s+1)(16.9688s+1)(17.375s+1)(77.5s+1)e^{-7.125s}}{(0.1133s+1)(0.25s+1)(23.7188s+1)(23.9999s+1)(24.2188s+1)(\tau_4 s+1)} \quad \text{(C3-13)}$$

$$C_{41,3} = \frac{-0.255607(-1.0625s+1)(-s+1)(5.125s+1)(16.9688s+1)(17.375s+1)}{(0.1133s+1)(0.25s+1)(18s+1)(19.75s+1)(20s+1)(\tau_1 s+1)} \quad \text{(C3-14)}$$

$$C_{42,3} = \frac{-0.0121119(-13.25s+1)(-9.75s+1)(-0.5s+1)(16.9688s+1)(17.375s+1)e^{-29.6855s}}{(0.1133s+1)(0.25s+1)(4.3828s+1)(10.5s+1)(22.0156s+1)(\tau_2 s+1)} \quad \text{(C3-15)}$$

$$C_{43,3} = \frac{0.00452948(1.0039s+1)(1.9373s+1)(16.9688s+1)(17.375s+1)}{(0.1133s+1)(0.25s+1)(s+0.0432123)(15.499s+1)(16.0156s+1)(\tau_3 s+1)} \quad \text{(C3-16)}$$

$$C_{44,3} = \frac{0.0816345(-1.375s+1)(-0.625s+1)(-0.25s+1)(16.9688s+1)(17.375s+1)}{(0.1133s+1)(0.25s+1)(18s+1)(19.9995s+1)(20.001s+1)(\tau_4 s+1)}. \quad \text{(C3-17)}$$

where as B5-2–B5-10, shown at the bottom of page 17.

APPENDIX B6: CONTROLLER MATRIX FOR ATDIMC DESIGN ACHIEVING "IMPERFECT y_2&y_3" FOR 3 × 3 DEPROPANIZER

Using the procedure in Section III-C ($j = 2, n = 3$), modified ATDIMC controllers achieving "imperfect y_2 & y_3" for 3×3 Depropanizer was computed as

$$C_{3\times 3.23}(s) = \begin{bmatrix} C_{11,23}(s) & C_{12,23}(s) & C_{13,23}(s) \\ C_{21,23}(s) & C_{22,23}(s) & C_{23,23}(s) \\ C_{31,23}(s) & C_{32,23}(s) & C_{33,23}(s) \end{bmatrix} \tag{B6-1}$$

where as B6-2–B6-10, shown at the bottom of page 17.

APPENDIX B7: CONTROLLER MATRIX FOR DYNAMIC DIMC DESIGN USING PROCEDURE IN [18] FOR 3 × 3 DEPROPANIZER

Using the procedure in [18], with the structure adopted being the IMC structure and the model simplification technique used being as described in Section IV of this paper, the dynamic decoupling internal model controller developed for comparison purposes is

$$C_{3\times 3,dd}(s) = \begin{bmatrix} C_{11,dd}(s) & C_{12,dd}(s) & C_{13,dd}(s) \\ C_{21,dd}(s) & C_{22,dd}(s) & C_{23,dd}(s) \\ C_{31,dd}(s) & C_{32,dd}(s) & C_{33,dd}(s) \end{bmatrix} \tag{B7-1}$$

where as B7-2–B7-10, shown at the bottom of page 18.

$$C_{11,4} = \frac{0.141506(-42.2836s+1)(16.9688s+1)(17.375s+1)e^{-10.5814s}}{(0.1133s+1)(0.25s+1)(18.3872s+1)(18.6942s+1)(\tau_1 s+1)} \tag{C4-2}$$

$$C_{12,4} = \frac{\begin{bmatrix} 0.0154741(-25.9887s+1)(-10.2656s+1)(-1.9412s+1)(-1.4979s+1) \\ (16.9688s+1)(17.375s+1) \end{bmatrix} e^{-11.6372s}}{(0.1133s+1)(0.25s+1)(10.4221s+1)(11.6229s+1)(12.6775s+1)(20.8565s+1)(\tau_2 s+1)} \tag{C4-3}$$

$$C_{13,4} = \frac{0.0310904(5.873s+1)(16.9688s+1)(17.375s+1)(119.5s+1)e^{-17.72s}}{(0.1133s+1)(0.25s+1)(14.5s+1)(22s+1)(\tau_3 s+1)} \tag{C4-4}$$

$$C_{14,4} = \frac{-0.0997113(-s+0.0432123)(1.6032s+1)(16.9688s+1)(17.375s+1)}{(0.1133s+1)(0.25s+1)(s+0.0432123)(14.3083s+1)(14.9843s+1)(\tau_4 s+1)} \tag{C4-5}$$

$$C_{21,4} = \frac{0.106285(-2.3971s+1)(-2.2659s+1)(-0.0625s+1)(16.97s+1)(17.375s+1)e^{-24.7031s}}{(0.1133s+1)(0.25s+1)(6s+1)(7s+1)(8s+1)(\tau_1 s+1)} \tag{C4-6}$$

$$C_{22,4} = \frac{-0.0616478(-2.2031s+1)(-1.6563s+1)(-0.1094s+1)(16.97s+1)(17.375s+1)e^{-26.29s}}{(0.1133s+1)(0.25s+1)(8.5s+1)(9s+1)(9.75s+1)(\tau_2 s+1)} \tag{C4-7}$$

$$C_{23,4} = \frac{0.021459(-1.1875s+1)(-1.1563s+1)(-1.125s+1)(16.97s+1)(17.375s+1)(52s+1)e^{-3s}}{(0.1133s+1)(0.25s+1)(6s+1)(8s+1)(10s+1)^2(\tau_3 s+1)} \tag{C4-8}$$

$$C_{24,4} = \frac{-0.0152609(-s+0.0432123)(-0.5s+1)^3(16.9688s+1)(17.375s+1)(18.0635s+1)e^{-32.4428s}}{(0.1133s+1)(0.25s+1)(s+0.0432123)(5.25s+1)(5.5s+1)(6.002s+1)(6.5s+1)(\tau_4 s+1)} \tag{C4-9}$$

$$C_{31,4} = \frac{0.177215(-3.5s+1)^2(16.9688s+1)(17.375s+1)(68.906s+1)}{(0.1133s+1)(0.25s+1)(20s+1)^2(22s+1)(\tau_1 s+1)} \tag{C4-10}$$

$$C_{32,4} = \frac{0.05332(0.5s+1)(16.9688s+1)(17.375s+1)(50.2656s+1)e^{-31.9583s}}{(0.1133s+1)(0.25s+1)(28.3125s+1)(29.125s+1)(\tau_2 s+1)} \tag{C4-11}$$

$$C_{33,4} = \frac{-0.0715523(-0.6406s+1)(-0.0293s+1)(16.9688s+1)(17.375s+1)(45s+1)}{(0.1133s+1)(0.25s+1)(9.75s+1)(10s+1)(20s+1)(\tau_3 s+1)} \tag{C4-12}$$

$$C_{34,4} = \frac{0.0402176(-s+0.0432123)(1.25s+1)(16.9688s+1)(17.375s+1)e^{-59.5665s}}{(0.1133s+1)(0.25s+1)(s+0.0432123)(8.0625s+1)(10s+1)(\tau_4 s+1)} \tag{C4-13}$$

$$C_{41,4} = \frac{-0.255607(-3.5059s+1)(1.5s+1)(16.9688s+1)(17.375s+1)e^{-14.4375s}}{(0.1133s+1)(0.25s+1)(14.0078s+1)(19.498s+1)(\tau_1 s+1)} \tag{C4-14}$$

$$C_{42,4} = \frac{-0.0121119(-4.9401s+1)(-4.908s+1)(-4.8946s+1)(-4.725s+1)(16.9688s+1)(17.375s+1)}{(0.1133s+1)(0.25s+1)(15.0116s+1)(15.0298s+1)(15.0422s+1)(24.9239s+1)(\tau_2 s+1)} \tag{C4-15}$$

$$C_{43,4} = \frac{0.104841(-1.625s+1)(-1.375s+1)(-1.1152s+1)(-s+1)(16.9688s+1)(17.375s+1)e^{-8s}}{(0.1133s+1)(0.25s+1)(5s+1)(6.5s+1)(11.75s+1)(13.125s+1)(\tau_3 s+1)} \tag{C4-16}$$

$$C_{44,4} = \frac{0.00352762(-0.9609s+1)(16.9688s+1)(17.375s+1)(60.0938s+1)e^{-35.57s}}{(0.1133s+1)(0.25s+1)(s+0.0432123)(8.8745s+1)(59.9998s+1)(\tau_4 s+1)}. \tag{C4-17}$$

APPENDIX B8: CONTROLLER MATRIX FOR MULTIVARIABLE PID DESIGN BY SIMPLIFIED DYNAMIC DECOUPLING USING PROCEDURE IN [20] FOR 3 × 3 DEPROPANIZER

Using the procedure for multivariable PID Design by Simplified Decoupling in [20], the authors presented the following controller for the 3 × 3 Depropanizer:

$$C_{3\times3,mvp}(s) = \begin{bmatrix} K_{11,mvp}(s) & K_{12,mvp}(s) & K_{13,mvp}(s) \\ K_{21,mvp}(s) & K_{22,mvp}(s) & K_{23,mvp}(s) \\ K_{31,mvp}(s) & K_{32,mvp}(s) & K_{33,mvp}(s) \end{bmatrix} \tag{B8-1}$$

where

$$K_{11,mvp} = 0.5072 + \frac{0.0056}{s} \tag{B8-2}$$

$$K_{12,mvp} = 0.0584 + \frac{0.005}{s} - \frac{3.68s}{13.89s+1} \tag{B8-3}$$

$$K_{13,mvp} = 0.1113 + \frac{0.0039}{s} \tag{B8-4}$$

$$K_{21,mvp} = 0.0301 + \frac{0.0013}{s} - \frac{4.456s}{44.35s+1} \tag{B8-5}$$

$$K_{22,mvp} = 0.0245 + \frac{0.0003}{s} \tag{B8-6}$$

$$K_{23,mvp} = 0.0032 + \frac{4.4\times10^{-4}}{s} + \frac{0.995s}{35.6s+1} \tag{B8-7}$$

$$K_{31,mvp} = 1.0293 + \frac{0.0214}{s} - \frac{76.5s}{83.35s+1} \tag{B8-8}$$

$$K_{32,mvp} = 0.2106 + \frac{0.0095}{s} + \frac{0.01s}{0.26s+1} \tag{B8-9}$$

$$K_{33,mvp} = 0.6 + \frac{0.0022}{s} + \frac{12.28s}{2.05s+1}. \tag{B8-10}$$

$$C_{11,12} = \frac{0.00611518(s+1)^2(16.9688s+1)(17.375s+1)e^{-5.2502s}}{(0.1133s+1)(0.25s+1)(s+0.0432123)(5.25s+1)(10.25s+1)(\tau_1 s+1)} \tag{C5-2}$$

$$C_{12,12} = \frac{0.000668673(-0.5002s+1)(16.9688s+1)(17.375s+1)(98s+1)e^{-2.9415s}}{(0.1133s+1)(0.25s+1)(s+0.0432123)(14.1249s+1)(14.7812s+1)(\tau_2 s+1)} \tag{C5-3}$$

$$C_{13,12} = \frac{0.0310904(1.9531s+1)(16.9688s+1)(17.375s+1)(54.0088s+1)}{(0.1133s+1)(0.25s+1)(11.7188s+1)(14.375s+1)(\tau_3 s+1)} \tag{C5-4}$$

$$C_{14,12} = \frac{-0.0997113(-6.8125s+1)(-3.2969s+1)(-2.3906s+1)(17.375s+1)(43.496s+1)}{(0.1133s+1)(0.25s+1)(11.9844s+1)(12.9688s+1)(18s+1)(\tau_4 s+1)} \tag{C5-5}$$

$$C_{21,12} = \frac{0.00459281(-4.8125s+1)(4.7548s+1)(16.9688s+1)(17.375s+1)e^{-12.51s}}{(0.1133s+1)(0.25s+1)(s+0.0432123)(6s+1)(6.2539s+1)(\tau_1 s+1)} \tag{C5-6}$$

$$C_{22,12} = \frac{-0.00266395(-9.6875s+1)(0.5s+1)(16.9688s+1)(17.375s+1)e^{-21.875s}}{(0.1133s+1)(0.25s+1)(s+0.0432123)(8.5s+1)(8.75s+1)(\tau_2 s+1)} \tag{C5-7}$$

$$C_{23,12} = \frac{0.021459(-183.608s+1)(-0.1011s+1)(4s+1)(16.9688s+1)(17.375s+1)e^{-33.87s}}{(0.1133s+1)(0.25s+1)(10s+1)(17.0938s+1)(17.3438s+1)(\tau_3 s+1)} \tag{C5-8}$$

$$C_{24,12} = \frac{-0.0152609(0.7495s+1)(16.9688s+1)(17.375s+1)(45.125s+1)(315s+1)e^{-29.82s}}{(0.1133s+1)(0.25s+1)(28s+1)^2(32s+1)(\tau_4 s+1)} \tag{C5-9}$$

$$C_{31,12} = \frac{0.00765788(s+1)(16.9688s+1)(17.375s+1)e^{-12.5007s}}{(0.1133s+1)(0.25s+1)(s+0.0432123)(136.813s^2+18.8438s+1)(\tau_1 s+1)} \tag{C5-10}$$

$$C_{32,12} = \frac{0.00230408(-5.75s+1)(7.25s+1)(16.9688s+1)(17.375s+1)}{(0.1133s+1)(0.25s+1)(s+0.0432123)(19.5s+1)(22.75s+1)(\tau_2 s+1)} \tag{C5-11}$$

$$C_{33,12} = \frac{-0.0715523(-33.5039s+1)(3s+1)(16.9688s+1)(17.375s+1)e^{-12.375s}}{(0.1133s+1)(0.25s+1)(25.7499s+1)(27s+1)(\tau_3 s+1)} \tag{C5-12}$$

$$C_{34,12} = \frac{0.0402176(16.9688s+1)(17.375s+1)(103.398s+1)e^{-18.1868s}}{(0.1133s+1)(0.25s+1)(30.5002s+1)(32.4985s+1)(\tau_4 s+1)} \tag{C5-13}$$

$$C_{41,12} = \frac{-0.0110499(0.2501s+1)(16.9688s+1)(17.375s+1)}{(0.1133s+1)(0.25s+1)(7.5s+1)(9.3124s+1)(\tau_1 s+1)} \tag{C5-14}$$

$$C_{42,12} = \frac{-0.000523385(s+1)(16.9688s+1)(17.375s+1)(129.875s+1)e^{-4.126s}}{(0.1133s+1)(0.25s+1)(s+0.0432123)(11.875s+1)(12.1875s+1)(\tau_2 s+1)} \tag{C5-15}$$

$$C_{43,12} = \frac{\begin{bmatrix} 0.104841(-1.6875s+1)(-1.6016s+1)(-1.3789s+1)(16.9688s+1) \\ (17.375s+1)(44.75s+1) \end{bmatrix} e^{-2.0156s}}{(0.1133s+1)(0.25s+1)(12.0898s+1)(12.4373s+1)(13.0938s+1)(14s+1)(\tau_3 s+1)} \tag{C5-16}$$

$$C_{44,12} = \frac{\begin{bmatrix} 0.0816345(-1.4531s+1)(-1.2263s+1)(-0.8513s+1)(16.9688s+1) \\ (17.375s+1)(48.0156s+1) \end{bmatrix} e^{-13.875s}}{(0.1133s+1)(0.25s+1)(11.4766s+1)(12.0625s+1)(13.0938s+1)(13.375s+1)(\tau_4 s+1)}. \tag{C5-17}$$

APPENDIX C
CONTROLLER MATRIX DETAILS FOR DESIGNS FOR THE 4 × 4 F4d2 SYSTEM OF [40]

APPENDIX C1: CONTROLLER MATRIX FOR ATDIMC DESIGN ACHIEVING "IMPERFECT y_1" FOR 4 × 4 F4d2 SYSTEM OF [40]

Using the procedure in Section III-B ($i = 1$), the ATDIMC controller achieving "imperfect y_1" for 4 × 4 F4d2 System was computed as

$$C_{4\times4,1}(s) = \begin{bmatrix} C_{11,1}(s) & C_{12,1}(s) & C_{13,1}(s) & C_{14,1}(s) \\ C_{21,1}(s) & C_{22,1}(s) & C_{23,1}(s) & C_{24,1}(s) \\ C_{31,1}(s) & C_{32,1}(s) & C_{33,1}(s) & C_{34,1}(s) \\ C_{41,1}(s) & C_{42,1}(s) & C_{43,1}(s) & C_{44,1}(s) \end{bmatrix} \tag{C1-1}$$

where as C1-2–C1-17, shown at the bottom of page 19.

APPENDIX C2: CONTROLLER MATRIX FOR ATDIMC DESIGN ACHIEVING "IMPERFECT y_2" FOR 4 × 4 F4d2 SYSTEM OF [40]

Using the procedure in Section III-B ($i = 2$), the ATDIMC controller achieving "imperfect y_2" for 4 × 4 F4d2 System was computed as

$$C_{4\times4,2}(s) = \begin{bmatrix} C_{11,2}(s) & C_{12,2}(s) & C_{13,2}(s) & C_{14,2}(s) \\ C_{21,2}(s) & C_{22,2}(s) & C_{23,2}(s) & C_{24,2}(s) \\ C_{31,2}(s) & C_{32,2}(s) & C_{33,2}(s) & C_{34,2}(s) \\ C_{41,2}(s) & C_{42,2}(s) & C_{43,2}(s) & C_{44,2}(s) \end{bmatrix} \tag{C2-1}$$

$$C_{11,32} = \frac{0.141506(-13.25s+1)(2.6565s+1)(16.9688s+1)(17.375s+1)(63s+1)e^{-2.2168s}}{(0.1133s+1)(0.25s+1)(19s+1)(19.875s+1)(20.3125s+1)(\tau_1 s+1)} \tag{C6-2}$$

$$C_{12,32} = \frac{0.000668673(-0.5002s+1)(16.9688s+1)(17.375s+1)(98s+1)e^{-2.9415s}}{(0.1133s+1)(0.25s+1)(s+0.0432123)(14.1249s+1)(14.7812s+1)(\tau_2 s+1)} \tag{C6-3}$$

$$C_{13,32} = \frac{0.00134349(-20s+1)(16.9688s+1)(17.375s+1)(29.0078s+1)e^{-37.4932s}}{(0.1133s+1)(0.25s+1)(s+0.0432123)(19.9961s+1)(23.7324s+1)(\tau_3 s+1)} \tag{C6-4}$$

$$C_{14,32} = \frac{-0.0997113(-6.8125s+1)(-3.2969s+1)(-2.3906s+1)(17.375s+1)(43.496s+1)}{(0.1133s+1)(0.25s+1)(11.9844s+1)(12.9688s+1)(18s+1)(\tau_4 s+1)} \tag{C6-5}$$

$$C_{21,32} = \frac{0.106285(5.9453s+1)(16.9688s+1)(17.375s+1)(137.477s+1)e^{-32.9666s}}{(0.1133s+1)(0.25s+1)(16.7344s+1)(19.5s+1)(\tau_1 s+1)} \tag{C6-6}$$

$$C_{22,32} = \frac{-0.00266395(-9.6875s+1)(0.5s+1)(16.9688s+1)(17.375s+1)e^{-21.875s}}{(0.1133s+1)(0.25s+1)(s+0.0432123)(8.5s+1)(8.75s+1)(\tau_2 s+1)} \tag{C6-7}$$

$$C_{23,32} = \frac{0.000927295(-7.5418s+1)(16.9688s+1)(17.375s+1)(60.1769s+1)e^{-43.6871s}}{(0.1133s+1)(0.25s+1)(s+0.0432123)(7.0857s+1)(59.912s+1)(\tau_3 s+1)} \tag{C6-8}$$

$$C_{24,32} = \frac{-0.0152609(0.7495s+1)(16.9688s+1)(17.375s+1)(45.125s+1)(315s+1)e^{-29.82s}}{(0.1133s+1)(0.25s+1)(28s+1)^2(32s+1)(\tau_4 s+1)} \tag{C6-9}$$

$$C_{31,32} = \frac{0.177215(-17.9999s+1)(0.5s+1)(16.9688s+1)(17.375s+1)e^{-5.4668s}}{(0.1133s+1)(0.25s+1)(26s+1)(30.25s+1)(\tau_1 s+1)} \tag{C6-10}$$

$$C_{32,32} = \frac{0.00230408(-5.75s+1)(7.25s+1)(16.9688s+1)(17.375s+1)}{(0.1133s+1)(0.25s+1)(s+0.0432123)(19.5s+1)(22.75s+1)(\tau_2 s+1)} \tag{C6-11}$$

$$C_{33,32} = \frac{-0.00309194(0.5s+1)(s+1)(16.9688s+1)(17.375s+1)e^{-21.75s}}{(0.1133s+1)(0.25s+1)(s+0.0432123)(21s+1)(21.993s+1)(\tau_3 s+1)} \tag{C6-12}$$

$$C_{34,32} = \frac{0.0402176(16.9688s+1)(17.375s+1)(103.398s+1)e^{-18.1868s}}{(0.1133s+1)(0.25s+1)(30.5002s+1)(32.4985s+1)(\tau_4 s+1)} \tag{C6-13}$$

$$C_{41,32} = \frac{\begin{bmatrix} -0.255712(-0.9941s+1)(-0.9531s+1)(-0.875s+1)(16.9688s+1) \\ (17.375s+1)(45.8906s+1) \end{bmatrix}}{(0.1133s+1)(0.25s+1)(11.5625s+1)(12.125s+1)(12.6328s+1)(14.0938s+1)(\tau_1 s+1)} \tag{C6-14}$$

$$C_{42,32} = \frac{-0.000523385(s+1)(16.9688s+1)(17.375s+1)(129.875s+1)e^{-4.126s}}{(0.1133s+1)(0.25s+1)(s+0.0432123)(11.875s+1)(12.1875s+1)(\tau_2 s+1)} \tag{C6-15}$$

$$C_{43,32} = \frac{0.00452948(1.0039s+1)(1.9373s+1)(16.9688s+1)(17.375s+1)}{(0.1133s+1)(0.25s+1)(s+0.0432123)(15.499s+1)(16.0156s+1)(\tau_3 s+1)} \tag{C6-16}$$

$$C_{44,32} = \frac{\begin{bmatrix} 0.0816345(-1.4531s+1)(-1.2263s+1)(-0.8513s+1)(16.9688s+1) \\ (17.375s+1)(48.0156s+1) \end{bmatrix} e^{-13.875s}}{(0.1133s+1)(0.25s+1)(11.4766s+1)(12.0625s+1)(13.0938s+1)(13.375s+1)(\tau_4 s+1)}. \tag{C6-17}$$

where as C2-2–C2-17, shown at the bottom of page 20.

where as C3-2–C3-17, shown at the bottom of page 21.

APPENDIX C3: CONTROLLER MATRIX FOR ATDIMC DESIGN ACHIEVING "IMPERFECT y_3" FOR 4 × 4 F4d2 SYSTEM OF [40]

Using the procedure in Section III-B ($i = 3$), the ATDIMC controller achieving "imperfect y_3" for 4 × 4 F4d2 System was computed as

$$C_{4\times4,3}(s) = \begin{bmatrix} C_{11,3}(s) & C_{12,3}(s) & C_{13,3}(s) & C_{14,3}(s) \\ C_{21,3}(s) & C_{22,3}(s) & C_{23,3}(s) & C_{24,3}(s) \\ C_{31,3}(s) & C_{32,3}(s) & C_{33,3}(s) & C_{34,3}(s) \\ C_{41,3}(s) & C_{42,3}(s) & C_{43,3}(s) & C_{44,3}(s) \end{bmatrix} \tag{C3-1}$$

APPENDIX C4: CONTROLLER MATRIX FOR ATDIMC DESIGN ACHIEVING "IMPERFECT y_4" FOR 4 × 4 F4d2 SYSTEM OF [40]

Using the procedure in Section III-A ($n = 4$), the ATDIMC controller achieving "imperfect y_4" for 4 × 4 F4d2 System was computed as

$$C_{4\times4,4}(s) = \begin{bmatrix} C_{11,4}(s) & C_{12,4}(s) & C_{13,4}(s) & C_{14,4}(s) \\ C_{21,4}(s) & C_{22,4}(s) & C_{23,4}(s) & C_{24,4}(s) \\ C_{31,4}(s) & C_{32,4}(s) & C_{33,4}(s) & C_{34,4}(s) \\ C_{41,4}(s) & C_{42,4}(s) & C_{43,4}(s) & C_{44,4}(s) \end{bmatrix} \tag{C4-1}$$

$$C_{11,42} = \frac{0.141506(-13.25s+1)(2.6565s+1)(16.9688s+1)(17.375s+1)(63s+1)e^{-2.2168s}}{(0.1133s+1)(0.25s+1)(19s+1)(19.875s+1)(20.3125s+1)(\tau_1 s+1)} \tag{C7-2}$$

$$C_{12,42} = \frac{0.000668673(-0.5002s+1)(16.9688s+1)(17.375s+1)(98s+1)e^{-2.9415s}}{(0.1133s+1)(0.25s+1)(s+0.0432123)(14.1249s+1)(14.7812s+1)(\tau_2 s+1)} \tag{C7-3}$$

$$C_{13,42} = \frac{0.0310904(1.9531s+1)(16.9688s+1)(17.375s+1)(54.0088s+1)}{(0.1133s+1)(0.25s+1)(11.7188s+1)(14.375s+1)(\tau_3 s+1)} \tag{C7-4}$$

$$C_{14,42} = \frac{-0.0997113(-s+0.0432123)(1.6032s+1)(16.9688s+1)(17.375s+1)}{(0.1133s+1)(0.25s+1)(s+0.0432123)(14.3083s+1)(14.9843s+1)(\tau_4 s+1)} \tag{C7-5}$$

$$C_{21,42} = \frac{0.106285(5.9453s+1)(16.9688s+1)(17.375s+1)(137.477s+1)e^{-32.9666s}}{(0.1133s+1)(0.25s+1)(16.7344s+1)(19.5s+1)(\tau_1 s+1)} \tag{C7-6}$$

$$C_{22,42} = \frac{-0.00266395(-9.6875s+1)(0.5s+1)(16.9688s+1)(17.375s+1)e^{-21.875s}}{(0.1133s+1)(0.25s+1)(s+0.0432123)(8.5s+1)(8.75s+1)(\tau_2 s+1)} \tag{C7-7}$$

$$C_{23,42} = \frac{0.021459(-183.608s+1)(-0.1011s+1)(4s+1)(16.9688s+1)(17.375s+1)e^{-33.87s}}{(0.1133s+1)(0.25s+1)(10s+1)(17.0938s+1)(17.3438s+1)(\tau_3 s+1)} \tag{C7-8}$$

$$C_{24,42} = \frac{-0.0152609(-s+0.0432123)(-0.5s+1)^3(16.9688s+1)(17.375s+1)(18.0635s+1)e^{-32.443s}}{(0.1133s+1)(0.25s+1)(s+0.0432123)(5.25s+1)(5.5s+1)(6s+1)(6.5s+1)(\tau_4 s+1)} \tag{C7-9}$$

$$C_{31,42} = \frac{0.177215(-17.9999s+1)(0.5s+1)(16.9688s+1)(17.375s+1)e^{-5.4668s}}{(0.1133s+1)(0.25s+1)(26s+1)(30.25s+1)(\tau_1 s+1)} \tag{C7-10}$$

$$C_{32,42} = \frac{0.00230408(-5.75s+1)(7.25s+1)(16.9688s+1)(17.375s+1)}{(0.1133s+1)(0.25s+1)(s+0.0432123)(19.5s+1)(22.75s+1)(\tau_2 s+1)} \tag{C7-11}$$

$$C_{33,42} = \frac{-0.0715523(-33.5039s+1)(3s+1)(16.9688s+1)(17.375s+1)e^{-12.375s}}{(0.1133s+1)(0.25s+1)(25.7499s+1)(27s+1)(\tau_3 s+1)} \tag{C7-12}$$

$$C_{34,42} = \frac{0.0402176(-s+0.0432123)(1.25s+1)(16.9688s+1)(17.375s+1)e^{-59.5665s}}{(0.1133s+1)(0.25s+1)(s+0.0432123)(8.0625s+1)(10s+1)(\tau_4 s+1)} \tag{C7-13}$$

$$C_{41,42} = \frac{\begin{bmatrix} -0.255712(-0.9941s+1)(-0.9531s+1)(-0.875s+1)(16.9688s+1) \\ (17.375s+1)(45.8906s+1) \end{bmatrix}}{(0.1133s+1)(0.25s+1)(11.5625s+1)(12.125s+1)(12.6328s+1)(14.0938s+1)(\tau_1 s+1)} \tag{C7-14}$$

$$C_{42,42} = \frac{-0.000523385(s+1)(16.9688s+1)(17.375s+1)(129.875s+1)e^{-4.126s}}{(0.1133s+1)(0.25s+1)(s+0.0432123)(11.875s+1)(12.1875s+1)(\tau_2 s+1)} \tag{C7-15}$$

$$C_{43,42} = \frac{\begin{bmatrix} 0.104841(-1.6875s+1)(-1.6016s+1)(-1.3789s+1)(16.9688s+1) \\ (17.375s+1)(44.75s+1) \end{bmatrix} e^{-2.0156s}}{(0.1133s+1)(0.25s+1)(12.0898s+1)(12.4373s+1)(13.0938s+1)(14s+1)(\tau_3 s+1)} \tag{C7-16}$$

$$C_{44,42} = \frac{0.00352762(-0.9609s+1)(16.9688s+1)(17.375s+1)(60.094s+1)e^{-35.57s}}{(0.1133s+1)(0.25s+1)(s+0.0432123)(8.8745s+1)(60s+1)(\tau_4 s+1)}. \tag{C7-17}$$

where as C4-2–C4-17, shown at the bottom of page 22.

APPENDIX C5: CONTROLLER MATRIX FOR ATDIMC DESIGN ACHIEVING "IMPERFECT y_1&y_2" FOR 4 × 4 F4d2 SYSTEM OF [40]

Using the procedure in Section III-D ($j = 1, i = 2$), the ATDIMC controller achieving "imperfect y_1&y_2" for 4 × 4 F4d2 System was computed as

$$C_{4\times4,12}(s) = \begin{bmatrix} C_{11,12}(s) & C_{12,12}(s) & C_{13,12}(s) & C_{14,12}(s) \\ C_{21,12}(s) & C_{22,12}(s) & C_{23,12}(s) & C_{24,12}(s) \\ C_{31,12}(s) & C_{32,12}(s) & C_{33,12}(s) & C_{34,12}(s) \\ C_{41,12}(s) & C_{42,12}(s) & C_{43,12}(s) & C_{44,12}(s) \end{bmatrix} \tag{C5-1}$$

where as C5-2–C5-17, shown at the bottom of page 23.

APPENDIX C6: CONTROLLER MATRIX FOR ATDIMC DESIGN ACHIEVING "IMPERFECT y_3&y_2" FOR 4 × 4 F4d2 SYSTEM OF [40]

Using the procedure in Section III-D ($j = 3, i = 2$), the ATDIMC controller achieving "imperfect y_1&y_2" for 4 × 4 F4d2 System was computed as

$$C_{4\times4,32}(s) = \begin{bmatrix} C_{11,32}(s) & C_{12,32}(s) & C_{13,32}(s) & C_{14,32}(s) \\ C_{21,32}(s) & C_{22,32}(s) & C_{23,32}(s) & C_{24,32}(s) \\ C_{31,32}(s) & C_{32,32}(s) & C_{33,32}(s) & C_{34,32}(s) \\ C_{41,32}(s) & C_{42,32}(s) & C_{43,32}(s) & C_{44,32}(s) \end{bmatrix} \tag{C6-1}$$

$$C_{11,dd} = \frac{0.00611518(-s+0.0432123)(s+1)^2(16.9688s+1)(17.375s+1)e^{-5.2502s}}{(0.1133s+1)(0.25s+1)(s+0.0432123)^2(5.25s+1)(10.25s+1)(\tau_1 s+1)} \tag{C8-2}$$

$$C_{12,dd} = \frac{0.000668673(-0.5002s+1)(-s+0.0432123)(16.97s+1)(17.375s+1)(98s+1)e^{-2.9415s}}{(0.1133s+1)(0.25s+1)(s+0.0432123)^2(14.1249s+1)(14.7812s+1)(\tau_2 s+1)} \tag{C8-3}$$

$$C_{13,dd} = \frac{0.00134349(-20s+1)(-s+0.0432123)(16.9688s+1)(17.375s+1)(29.0078s+1)}{(0.1133s+1)(0.25s+1)(s+0.0432123)^2(19.9961s+1)(23.7324s+1)(\tau_3 s+1)} \tag{C8-4}$$

$$C_{14,dd} = \frac{-0.0997113(-s+0.0432123)^2(1.6032s+1)(16.9688s+1)(17.375s+1)}{(0.1133s+1)(0.25s+1)(s+0.0432123)^2(14.31s+1)(14.9843s+1)(\tau_4 s+1)} \tag{C8-5}$$

$$C_{21,dd} = \frac{0.00459281(-4.8125s+1)(-s+0.0432123)(4.7548s+1)(16.9688s+1)(17.375s+1)e^{-12.51s}}{(0.1133s+1)(0.25s+1)(s+0.0432123)^2(6s+1)(6.2539s+1)(\tau_1 s+1)} \tag{C8-6}$$

$$C_{22,dd} = \frac{-0.00266395(-9.6875s+1)(-s+0.0432123)(0.5s+1)(16.9688s+1)(17.375s+1)e^{-21.875s}}{(0.1133s+1)(0.25s+1)(s+0.0432123)^2(8.5s+1)(8.75s+1)(\tau_2 s+1)} \tag{C8-7}$$

$$C_{23,dd} = \frac{0.000927295(-7.5418s+1)(-s+0.0432123)(16.9688s+1)(17.375s+1)e^{-43.6871s}}{(0.1133s+1)(0.25s+1)(s+0.0432123)^2(7.0857s+1)(59.912s+1)(\tau_3 s+1)} \tag{C8-8}$$

$$C_{24,dd} = \frac{-0.015261(-s+0.0432123)^2(-0.5s+1)^3(16.9688s+1)(17.375s+1)(18.0635s+1)e^{-32.443s}}{(0.1133s+1)(0.25s+1)(s+0.0432123)^2(5.25s+1)(5.5s+1)(6.002s+1)(6.5s+1)(\tau_4 s+1)} \tag{C8-9}$$

$$C_{31,dd} = \frac{0.00765788(-s+0.0432123)(s+1)(16.9688s+1)(17.375s+1)e^{-12.5007s}}{(0.1133s+1)(0.25s+1)(s+0.0432123)^2(136.813s^2+18.8438s+1)(\tau_1 s+1)} \tag{C8-10}$$

$$C_{32,dd} = \frac{0.00230408(-5.75s+1)(-s+0.0432123)(7.25s+1)(16.9688s+1)(17.375s+1)}{(0.1133s+1)(0.25s+1)(s+0.0432123)^2(19.5s+1)(22.75s+1)(\tau_2 s+1)} \tag{C8-11}$$

$$C_{33,dd} = \frac{-0.00309194(-s+0.0432123)(0.5s+1)(s+1)(16.9688s+1)(17.375s+1)e^{-21.75s}}{(0.1133s+1)(0.25s+1)(s+0.0432123)^2(21s+1)(21.9927s+1)(\tau_3 s+1)} \tag{C8-12}$$

$$C_{34,dd} = \frac{0.0402176(-s+0.0432123)^2(1.25s+1)(16.9688s+1)(17.375s+1)e^{-59.57s}}{(0.1133s+1)(0.25s+1)(s+0.0432123)^2(8.0625s+1)(10s+1)(\tau_4 s+1)} \tag{C8-13}$$

$$C_{41,dd} = \frac{-0.0110499(-s+0.0432123)(0.2501s+1)(16.9688s+1)(17.375s+1)}{(0.1133s+1)(0.25s+1)(s+0.0432123)^2(7.5s+1)(9.3124s+1)(\tau_1 s+1)} \tag{C8-14}$$

$$C_{42,dd} = \frac{-0.00052339(-s+0.0432123)(s+1)(16.97s+1)(17.375s+1)(129.875s+1)e^{-4.13s}}{(0.1133s+1)(0.25s+1)(s+0.0432123)^2(11.875s+1)(12.1875s+1)(\tau_2 s+1)} \tag{C8-15}$$

$$C_{43,dd} = \frac{0.00452948(-s+0.0432123)(1.0039s+1)(1.9373s+1)(16.9688s+1)(17.375s+1)}{(0.1133s+1)(0.25s+1)(s+0.0432123)^2(15.499s+1)(16.0156s+1)(\tau_3 s+1)} \tag{C8-16}$$

$$C_{44,dd} = \frac{0.00352762(-s+0.0432123)(-0.96s+1)(16.9688s+1)(17.375s+1)(60.094s+1)e^{-35.57s}}{(0.1133s+1)(0.25s+1)(s+0.0432123)^2(8.8745s+1)(59.9998s+1)(\tau_4 s+1)}. \tag{C8-17}$$

where as C6-2–C6-17, shown at the bottom of page 24.

APPENDIX C7: CONTROLLER MATRIX FOR ATDIMC DESIGN ACHIEVING "IMPERFECT y_4&y_2" FOR 4 × 4 F4d2 SYSTEM OF [40]

Using the procedure in Section III-D ($j = 4, i = 2$), the ATDIMC controller achieving "imperfect y_1&y_2" for 4 × 4 F4d2 System was computed as

$$C_{4\times4,42}(s) = \begin{bmatrix} C_{11,42}(s) & C_{12,42}(s) & C_{13,42}(s) & C_{14,42}(s) \\ C_{21,42}(s) & C_{22,42}(s) & C_{23,42}(s) & C_{24,42}(s) \\ C_{31,42}(s) & C_{32,42}(s) & C_{33,42}(s) & C_{34,42}(s) \\ C_{41,42}(s) & C_{42,42}(s) & C_{43,42}(s) & C_{44,42}(s) \end{bmatrix} \tag{C7-1}$$

where as C7-2–C7-17, shown at the bottom of page 25.

APPENDIX C8: CONTROLLER MATRIX FOR DYNAMIC DIMC DESIGN USING PROCEDURE IN [18] FOR 4 × 4 F4d2 System Of [40]

Using the procedure in [18], with the structure adopted being the IMC structure and the model simplification technique used being as described in Section IV of this paper, the dynamic decoupling internal model controller developed for the 4 × 4 F4d2 System of [40] is:

$$C_{4\times4,dd}(s) = \begin{bmatrix} C_{11,dd}(s) & C_{12,dd}(s) & C_{13,dd}(s) & C_{14,dd}(s) \\ C_{21,dd}(s) & C_{22,dd}(s) & C_{23,dd}(s) & C_{24,dd}(s) \\ C_{31,dd}(s) & C_{32,dd}(s) & C_{33,dd}(s) & C_{34,dd}(s) \\ C_{41,dd}(s) & C_{42,dd}(s) & C_{43,dd}(s) & C_{44,dd}(s) \end{bmatrix} \tag{C8-1}$$

where as C8-2–C8-17, shown at the bottom of page 26.

ACKNOWLEDGMENT

The authors gratefully acknowledge the useful technical insights provided by Prof. Aleksandar Zecevic and Dr. Maryam Khanbaghi of the Department of Electrical and Computer Engineering, Santa Clara University.

REFERENCES

[1] C. E. Garcia and M. Morari, "Internal model control. A unifying review and some new results," *Ind. Eng. Chem. Process Design Develop.*, vol. 21, no. 2, pp. 308–323, Apr. 1982.

[2] C. E. Garcia and M. Morari, "Internal model control. 2. Design procedure for multivariable systems," *Ind. Eng. Chem. Process Design Develop.*, vol. 24, no. 2, pp. 472–484, Apr. 1985.

[3] M. Morari and E. Zafiriou, *Robust Process Control*. Englewood Cliffs, NJ, USA: Prentice-Hall, 1989.

[4] D. E. Rivera, M. Morari, and S. Skogestad, "Internal model control: PID controller design," *Ind. Eng. Chem. Process Design Develop.*, vol. 25, no. 1, pp. 252–265, 1986.

[5] G. E. Rotstein and D. R. Lewin, "Simple PI and PID tuning for open-loop unstable systems," *Ind. Eng. Chem. Res.*, vol. 30, no. 8, pp. 1864–1869, Aug. 1991.

[6] Y. Lee, J. Lee, and S. Park, "PID controller tuning for integrating and unstable processes with time delay," *Chem. Eng. Sci.*, vol. 55, no. 17, pp. 3481–3493, Sep. 2000.

[7] C. G. Economou, M. Morari, and B. O. Palsson, "Internal model control: Extension to nonlinear systems," *Ind. Eng. Chem. Process Design Develop.*, vol. 25, no. 2, pp. 403–411, 1986.

[8] M. A. Henson and D. E. Seborg, "An internal model control strategy for nonlinear systems," *AIChE J.*, vol. 37, no. 7, pp. 1065–1081, Jul. 1991.

[9] C. E. Garcia and M. Morari, "Internal model control. 3. Multivariable control law computation and tuning guidelines," *Ind. Eng. Chem. Process Design Develop.*, vol. 24, no. 2, pp. 484–494, Apr. 1985.

[10] C. G. Economou and M. Morari, "Internal model control: Multiloop design," *Ind. Eng. Chem. Process Design Develop.*, vol. 25, no. 2, pp. 411–419, Apr. 1986.

[11] Q.-G. Wang, Y. Zhang, and M.-S. Chiu, "Decoupling internal model control for multivariable systems with multiple time delays," *Chem. Eng. Sci.*, vol. 57, no. 1, pp. 115–124, Jan. 2002.

[12] Q. G. Wang, C. C. Hang, and X. P. Yang, "IMC-based controller design for MIMO systems," *J. Chem. Eng. Jpn.*, vol. 35, no. 12, pp. 1231–1243, 2002b.

[13] Q. G. Wang, *Decoupling Control*. New York, NY, USA: Springer-Verlag, 2003.

[14] T. Liu, W. Zhang, and D. Gu, "Analytical design of decoupling internal model control (IMC) scheme for Two-Input-Two-Output (TITO) processes with time delays," *Ind. Eng. Chem. Res.*, vol. 45, no. 9, pp. 3149–3160, Apr. 2006.

[15] J. Garrido, F. Vázquez, and F. Morilla, "Inverted decoupling internal model control for square stable multivariable time delay systems," *J. Process Control*, vol. 24, no. 11, pp. 1710–1719, Nov. 2014.

[16] S. Skogestad and I. Postlethwaite, *Multivariable Feedback Control: Analysis and Design*, 2nd ed. Chichester, U.K.: Wiley, 2005.

[17] M. Waller, J. B. Waller, and K. V. Waller, "Decoupling revisited," *Ind. Eng. Chem. Res.*, vol. 42, no. 20, pp. 4575–4577, Jul. 2003.

[18] T. Liu, W. Zhang, and F. Gao, "Analytical decoupling control strategy using a unity feedback control structure for MIMO processes with time delays," *J. Process Control*, vol. 17, no. 2, pp. 173–186, Feb. 2007.

[19] J. Garrido, F. Vázquez, and F. Morilla, "An extended approach of inverted decoupling," *J. Process Control*, vol. 21, no. 1, pp. 55–68, Jan. 2011.

[20] J. Garrido, F. Vázquez, and F. Morilla, "Centralized multivariable control by simplified decoupling," *J. Process Control*, vol. 22, no. 6, pp. 1044–1062, Jul. 2012.

[21] J. Garrido, F. Vázquez, and F. Morilla, "Centralized inverted decoupling control," *Ind. Eng. Chem. Res.*, vol. 52, no. 23, pp. 7854–7866, Jun. 2013.

[22] X. Luan, Q. Chen, P. Albertos, and F. Liu, "Compensator design based on inverted decoupling for non-square processes," *IET Control Theory Appl.*, vol. 11, no. 7, pp. 996–1005, Apr. 2017.

[23] Z. Zhou, S. Lin, G. Zhang, and W. Zhang, "Block inverted decoupling control with internal model structure for non-square multivariable time delay systems," *IFAC Papers Online*, vol. 50, no. 1, pp. 3617–3622, 2017.

[24] K. Liu and J. Chen, "Internal model control design based on equal order fractional Butterworth filter for multivariable systems," *IEEE Access*, vol. 8, pp. 84667–84679, 2020, doi: 10.1109/ACCESS.2020.2992598.

[25] B. R. Holt and M. Morari, "Design of resilient processing plants—VI. The effect of right-half-plane zeros on dynamic resilience," *Chem. Eng. Sci.*, vol. 40, no. 1, pp. 59–74, 1985.

[26] G. C. Goodwin, S. F. Graebe, and M. E. Salgado, *Control System Design*. Englewood Cliffs, NJ, USA: Prentice-Hall, 2000.

[27] A. S. Morse and W. M. Wonham, "Triangular decoupling of linear multivariable systems," *IEEE Trans. Autom. Control*, vol. AC-15, no. 4, pp. 447–449, Aug. 1970.

[28] S. H. Wang, "Relationship between triangular decoupling and invertibility of linear multivariate systems," *Int. J. Control*, vol. 15, no. 2, pp. 395–399, Feb. 1972.

[29] J. Descusse and R. Lizarzaburu, "Triangular decoupling and pole placement in linear multivariable systems: A direct algebraic approach," *Int. J. Control*, vol. 30, no. 1, pp. 139–152, Jul. 1979.

[30] H. Nijmeijer, "The triangular decoupling problem for nonlinear control systems," *Nonlinear Anal., Theory, Methods Appl.*, vol. 8, no. 3, pp. 273–279, Mar. 1984.

[31] F. N. Koumboulis and M. G. Skarpetis, "Robust triangular decoupling via output feedback," *J. Franklin Inst.*, vol. 337, no. 1, pp. 11–20, Jan. 2000.

[32] F. N. Koumboulis and G. E. Panagiotakis, "Transfer matrix approach to the triangular decoupling of general neural multi-delay systems," in *Proc. 17th IFAC World Congr.*, Seoul, South Korea, Jul. 2008, pp. 1–11.

[33] H. T. Nguyen and S. W. Su, "Conditions for triangular decoupling control," *Int. J. Control*, vol. 82, no. 9, pp. 1575–1581, Sep. 2009.

[34] D. Shen and M. Wei, "The pole assignment for the regular triangular decoupling problem," *Automatica*, vol. 53, pp. 208–215, Mar. 2015.

[35] M. Li, Y. Jia, and H. Liu, "Static state feedback triangular block decoupling for arbitrary systems: A state-space method," *Int. J. Control*, vol. 90, no. 7, pp. 1428–1436, Jul. 2017.
[36] F. N. Koumboulis and N. D. Kouvakas, "Delayless controllers for triangular decoupling with simultaneous disturbance rejection of general neutral time delay systems," in *Proc. 26th Medit. Conf. Control Autom. (MED)*, Zadar, Croatia, Jun. 2018, pp. 741–746.
[37] K. S. Ogunba, D. Fasiku, A. A. Fakunle, and O. Taiwo, "Analytical triangular decoupling internal model control of a class of two-input, two-output (TITO) systems with delays," *IFAC-PapersOnLine*, vol. 53, no. 2, pp. 4774–4779, 2020.
[38] E. Kreyszig, *Advanced Engineering Mathematics*, 9th ed. Hoboken, NJ, USA: Wilen, 2006.
[39] R. Pintelon, P. Guillaume, Y. Rolain, J. Schoukens, and H. Van Hamme, "Parametric identification of transfer functions in the frequency domain—A survey," *IEEE Trans. Autom. Control*, vol. 39, no. 11, pp. 2245–2260, Nov. 1994.
[40] K. S. Ogunba, "Internal-model-based formulations for control system design," Ph.D. thesis, Dept. Electron. Elect. Eng., Obafemi Awolowo Univ., Ile-Ife, Nigeria, 2021.

KOLAWOLE S. OGUNBA received the B.Sc. degree in electronic and electrical engineering, the M.Sc. degree in electronic and electrical engineering (specialization: control engineering), and the Ph.D. degree in control engineering from Obafemi Awolowo University, Ife, Nigeria, in 2004, 2012, and 2021, respectively.

He is currently a Postdoctoral Fellow with Santa Clara University, CA, USA. He has published three articles at international conferences. His current research interests include multivariable control system design, process control, laboratory-scale control, industrial control, adaptive signal processing, machine-learning techniques, and control of electric power systems.

AFEEZ A. FAKUNLE received the B.Sc. degree in electronic and electrical engineering from Obafemi Awolowo University, Ife, Nigeria, in 2019. He is currently pursuing the M.S. degree with the Department of Electrical and Computer Engineering, Santa Clara University, Santa Clara, CA, USA.

He has published an article at an international conference and two articles in international journals. His current research interests include robotics, control theory, adaptive signal processing, and machine-learning techniques.

TOKUNBO OGUNFUNMI received the B.S. degree (Hons.) in electrical engineering from Obafemi Awolowo University (formerly University of Ife), Ife, Nigeria, and the M.S. and Ph.D. degrees in electrical engineering from Stanford University, Stanford, CA, USA.

He is currently a Professor of electrical and computer engineering and the Director of the Information Processing and Machine Learning Research Laboratory, Santa Clara University (SCU), Santa Clara, CA, USA. From 2010 to 2014, he served as an Associate Dean for Research and Faculty Development, SCU School of Engineering. At SCU, he teaches a variety of courses in circuits, systems, signal processing, and related areas. He has published over 200 refereed journal and conference papers. His current research interests include digital and adaptive signal processing and applications, machine learning, deep learning, speech and multimedia (audio, video) compression, and nonlinear signal processing.

Prof. Ogunfunmi is currently serving on the Editorial Board for the IEEE TRANSACTIONS ON SIGNAL PROCESSING and the *Circuits, Systems and Signal Processing* (CSSP) journal. He has been involved with several IEEE conference committees as a member of the organizing and technical committees. He served as the General Chair for the 2018 IEEE Workshop on Signal Processing Systems (SiPS 2018) and the Technical Program Co-Chair for the 2019 IEEE International Symposium on Circuits and Systems (ISCAS 2019). He has served as a Visiting Professor with the University of Texas, Stanford University, and as a Carnegie Foundation Visiting Professor. He served the IEEE as a Distinguished Lecturer for the Circuits and Systems Society, from 2013 to 2014. He also served as a Lead Guest Editor for the *CSSP* journal Special Issue on "Algorithms and Architectures for Machine Learning based Speech Processing," published in August 2019, and a Lead Guest Editor for the *Journal of Signal Processing Systems* (JSPS) journal Special Issue on 2018 IEEE Workshop on Signal Processing Systems (SiPS).

OLUWAFEMI TAIWO received the B.Sc. degree in chemical engineering from University College, London, in 1974, and the M.Sc. and Ph.D. degrees in chemical engineering/theory and practice of automatic control from the University of Manchester Institute of Science and Technology (UMIST), Manchester, U.K., in 1975 and 1979, respectively.

He is currently a Professor of chemical engineering with the Process Systems Engineering Laboratory, Department of Chemical Engineering, Obafemi Awolowo University, Ife, Nigeria. He has over 90 publications in peer-reviewed journals in his area of research and international conferences. His research interests include process systems engineering, multivariable control, optimization-based engineering techniques, reliability engineering, multimodel control, generalization of internal model control, and numerical computation.

Prof. Taiwo is a fellow of the Nigerian Academy of Engineering, the Institution of Chemical Engineers, U.K., and the Nigerian Society of Engineers. He is currently the President of the Society for Automation, Control and Instrumentation of Nigeria. He has received several awards and benefited from several fellowships, including the British Council Fellowship, UMIST, in 1984; the Alexander von Humboldt Scholarship, Karlsruhe, Germany, in 1992; the Alexander von Humboldt Fellowship, Berlin, Germany, in 2000; the Alexander von Humboldt Fellowship, Clausthal-Zellerfeld, Germany, in 2005; the Erskine Fellowship, Christchurch, New Zealand, in 2008; and Alexander von Humboldt Fellowship, TUBerlin, in 2021.